Applied Mathematics and Computation 273 (2016) 1059–1089

Contents lists available at ScienceDirect

Applied Mathematics and Computation

journal homepage: www.elsevier.com/locate/amc

Mathematical insights and integrated strategies for the control of *Aedes aegypti* mosquito

Hong Zhang [a,b], Paul Georgescu [c,*], Adamu Shitu Hassan [b,d]

[a] Department of Financial Mathematics, Jiangsu University, Zhenjiang 212013, China
[b] Department of Mathematics and Applied Mathematics, University of Pretoria, Private Bag X20, Hatfield 0002, South Africa
[c] Department of Mathematics, Technical University of Iași, Bd. Copou 11, Iași 700506, Romania
[d] Department of Mathematical Sciences, Bayero University, PMB 3011, Kano, Nigeria

ARTICLE INFO

Keywords:
Sterile insect release
Stability of equilibria
Nonstandard finite difference (NFSD) scheme
Delay
Hopf bifurcation
Optimal control

ABSTRACT

This paper proposes and investigates a delayed model for the dynamics and control of a mosquito population which is subject to an integrated strategy that includes pesticide release, the use of mechanical controls and the use of the sterile insect technique (SIT). The existence of positive equilibria is characterized in terms of two threshold quantities, being observed that the "richer" equilibrium (with more mosquitoes in the aquatic phase) has better chances to be stable, while a longer duration of the aquatic phase has the potential to destabilize both equilibria. It is also found that the stability of the trivial equilibrium appears to be mostly determined by the value of the maturation rate from the aquatic phase to the adult phase.

A nonstandard finite difference (NSFD) scheme is devised to preserve the positivity of the approximating solutions and to keep consistency with the continuous model. The resulting discrete model is transformed into a delay-free model by using the method of augmented states, a necessary condition for the existence of optimal controls then determined. The particularities of different control regimes under varying environmental temperature are investigated by means of numerical simulations. It is observed that a combination of all three controls has the highest impact upon the size of the aquatic population. At higher environmental temperatures, the oviposition rate is seen to possess the most prominent influence upon the outcome of the control measures.

1. Introduction

Certain deadly infectious diseases, such as dengue fever [29,60], yellow fever [30] and malaria [49] are transmitted by mosquito species within the genus *Aedes*, principally by *Aedes aegypti* (the yellow fever mosquito) and *Aedes albopictus* (the Asian tiger mosquito). Among these species, *Aedes aegypti* is a small-to-medium sized (4 to 7 mm in its adult stage) dark mosquito, recognizable by the white markings on its legs and by the marking in the form of a lyre on its thorax, which is globally the main vector for the transmission of yellow fever and dengue fever. In Asia, it is the main vector of the chikungunya disease as well. The viruses carried by this species are passed on to humans through the bites of infective females, which acquire the viruses by feeding on the blood of infected persons. Recent estimates [8] indicate that, annually, there are 300–500 million cases of malaria

* Corresponding author. Tel.: +40 232 213737.
E-mail addresses: hongzhang@ujs.edu.cn (H. Zhang), v.p.georgescu@gmail.com (P. Georgescu), Adamu.Hassan@tuks.co.za (A.S. Hassan).

http://dx.doi.org/10.1016/j.amc.2015.10.066
0096-3003/

leading to more than 1 million deaths and 50–100 million cases of dengue fever [31]. In the absence of any intervention, the incidence of mosquito-borne diseases is expected to double in the next 10 years [8].

Humans provide mosquitoes not only with blood meals necessary to produce eggs, but also with water-filled artificial habitats (used tires, flower pots, animal drinking pans, trash cans, toilets and septic tanks). It has been determined that most female mosquitoes spend their entire lifetime in or around the dwellings they emerge as adults, flying an average of 400 m, which means that people, rather than mosquitoes, are mostly responsible for the movement of viruses between communities [36].

It is difficult to contain the expansion of *Aedes aegypti* mosquitoes since they have developed highly successful mechanisms to cope with a variable environment. Notably, the eggs have the ability to withstand desiccation for several months on the inner walls of containers and hatch once submerged in water. At first, massive insecticide use has been proved successful, generally limiting the spread of mosquito-borne diseases and even eradicating malaria in certain areas. However, these diseases are now resurgent largely since mosquitoes have developed insecticide resistance [44] while the areal of the vector and virus have also been expanding [46].

The unavailability of effective vaccines has also hampered the efforts to contain these diseases, although much effort has been put into developing suitable vaccine candidates. Only one vaccine candidate for dengue fever, a live-attenuated tetravalent vaccine based on chimeric yellow fever-dengue virus (CYD-TDV) developed by Sanofi-Pasteur has progressed to phase III clinical trials. The first of two pivotal efficacy studies has been conducted and completed as a multicenter, randomized, observer-masked, placebo-controlled trial in 2014 in five Asian countries [11,51]. Also, only one candidate vaccine for malaria, RTS, S/AS01 (Mosquirix, developed by Glaxo-SmithKline Inc.) reached phase III clinical trials, a randomized, controlled, double-blind trial being conducted at 11 sites in seven African countries [58,63]. Although the live chikungunya virus vaccine candidate TSI-GSD-218, developed by US Army Medical Research Institute, has undergone a phase 2 clinical study, appearing to be safe in human subjects, its development has been halted in 2003. To date, there is no vaccine that reached phase 2 of clinical trials [45,53,61]. Consequently, vector control remains a vital part of the ongoing global strategy for the control of mosquito-associated diseases.

The most common vector control mechanism is pesticide spraying (specifically, adulticides or larvicides, depending on the concrete situation), which can have a powerful impact on the abundance of mosquitoes. Four classes of insecticides are recommended by World Health Organization (WHO) to be used for public health purposes (pyrethroids, organochlorines, organophosphates and carbamates). However, the long term usage of pesticides has been shown to induce resistance in mosquitoes, thereby reducing pesticide efficiency, and to have a negative impact upon the other species that share the same habitat.

Another effective control mechanism is source reduction, by means of eliminating mosquito breeding areas. Since mosquitoes breed in stagnant water, this amounts to removing old tires and emptying buckets, clearing clogged gutters and repairing leaks around faucets, regularly changing water in animal drinking pans and draining puddles and swampy areas. Also, open water marsh management, which amounts to building a network of ditches to create water flows between marshes and letting fish in, which will then feed on mosquito larvae, is an effective way of reducing mosquito populations without resorting to insecticides.

Biological control methods rely upon using parasites or predators of mosquitoes to reduce the size of mosquito populations. Effective control agents include predatory fish and dragonflies that feed on larvae or adult mosquito populations. Bacteria such as *Bacillus thuringiensis*, which interfere with the digestive processes of larvae, and fungi such as *Metarhizium anisopliae* and *Beauveria bassiana*, which infect feeding and respiratory apparatus of larvae, reducing their chances of survival are also use.

Another approach is the breeding of sterile male mosquitoes, which are then subsequently released into the environment, interfering with the reproductive processes of wild mosquitoes, procedure called the sterile insect technique (SIT). The concept of SIT was first proposed by Knipling [37] in 1955, and successfully tested in 1958 in Florida to control Screwworm fly [38,39]. Over the past few years, there has been a growing realization that the SIT could play an important role in mosquito control under specific conditions [1,7,9,52,57], as a cheaper and effective control technique which is not subject to vector resistance.

One way of achieving the sterilization of mosquitoes is by exposing them to gamma radiations. It has been reported that many insects are difficult to sterilize without drastically affecting their fitness [64]. However, small scale experiments to assert survival fitness and mating competitiveness have been performed upon sterilized *Anopheles arabiensis* mosquitoes near Khartoum, Sudan, under near-natural conditions and are described in [33]. It appeared that the irradiation did not impact on first nights survival, which are crucial for reproduction, mating occurred in high frequencies and sterile mosquitoes were able to inseminate wild females at rates comparable to those of the wild males. Again in a small-scale experiment, it has been observed that the spermless *Anopheles gambiae* males developed by manipulation of germ cells differentiation gene elicit the same mating response from wild females [57]. Specifically, mating with sterile males does not affect female egg-laying and stimulus to mate for a second time (usually, a female mosquito mates only once in its lifetime).

Recently, mathematical models for the interaction between sterile and wild mosquitoes have been developed by several authors. Dumont and Tchuenche [20] considered the case of pulsed release of sterile mosquitoes, proving by means of an equilibrium analysis augmented by numerical simulations that frequent small releases of sterile insects are more effective than larger less frequent releases. Dumont and Dufourd [19] developed a mathematical model with pulsed release of sterile males to simulate mosquito dispersal and studied its controllability taking into account the variability of environmental parameters. Esteva and Yang [22] employed optimal control methods to find the appropriate rate for the introduction of sterile mosquitoes. Li [41,42] developed difference and respectively, differential models to characterize the interactions between wild and transgenic mosquitoes. Diaz *et al.* [17] analyzed a model that described the dynamics of gene selection under sexual reproduction in a closed vector population. Anguelov *et al.* [5] studied the dynamics of the equilibria for a SIT model dealing with the interaction between treated males and wild female anopheles by using the theory of monotone operators. Rafikov *et al.* [54,55] used an optimal control approach to determine the suitable release frequency of transgenic mosquitoes. Also, Fister *et al.* [24] considered an optimal

control framework for an ODE model to subsequently investigate the release of sterile mosquitoes with the purpose of reducing the incidence of mosquito-borne diseases.

However, to the best of our knowledge, none of these models incorporate delay and combine more than one control to determine the optimal strategies amongst them. When modeling the transmission of vector-borne diseases such as malaria, dengue fever or chikungunya fever, time delays may be incorporated in order to accurately represent the fact that the vectors become able to transmit the disease only after they reach certain developmental stages, see for example [15,23,50], or after a period of incubation. That is, time delays caused by the development of the disease-carrying vectors are actually integral parts of the process of disease transmission. Other types of delays, such as those caused by the viral replication processes, may also need to be accounted for. However, the introduction of time delays usually increases drastically the complexity of the mathematical apparatus involved and of the resulting behavior of the system, potentially leading to solutions that exhibit sustained or transient oscillations, or even chaotic behavior.

Two types of delays are usually employed in the modeling literature, namely discrete (constant) delays and continuously distributed delays, the latter especially when dealing with age structures for the host population such as age of infection or physical age. The use of continuously distributed delays usually leads to models involving partial differential equations or integrodifferential equations, whose treatment is significantly more challenging than the treatment of a model involving ordinary differential equations.

A competitive exclusion principle in a vector-host epidemic model with distributed delay has been established in Cai *et al.* [10]. It has been shown that in a multi-strain vector-borne model, the strain that maximizes both the vector and the human reproduction numbers dominates in the population, outcompeting all other strains. A model for the spread of an epidemic with both vector-mediated and direct transmission has been studied in Wei *et al.* [62]. Thus, it has been shown that the introduction of a time delay in the host-to-vector transmission term may destabilize the system and lead to the onset of periodic solutions through Hopf bifurcations. Global stability results for general host-vector models with continuously distributed delays expressing different types of age dependencies have been obtained by Lyapunov's direct method in Vargas-De-León *et al.* [59].

In this work, we are concerned with the optimal strategies for controlling the size of an *Aedes aegypti* mosquito population by means of three control mechanisms, namely the release of pesticides, the use of mechanical controls and the use of SIT. In order to shed further light on the effectiveness of the control techniques, we propose a model that incorporates two life phases of the mosquito population, namely the aquatic phase, which includes the egg, larva and pupa stages, and the adult phase. Since the first three aquatic stages typically last 5–14 days or even several weeks, we then assume that mosquito population resides in the aquatic compartment τ units of time. We also consider two factors that are particularly relevant to the application of control mechanisms, as indicated below.

(a) Ambient temperature has an important effect on the oviposition rate of the mosquitoes, the carrying capacity of the breeding sites, and the time spent in the aquatic phase [19,43,65].
(b) Pesticides have a residual effect, which weakens due to the degradation of the pesticide and natural clearance [56].

It is well known that it is difficult, if not downright impossible, to determine the exact solutions of most relevant nonlinear biological ODE and delay differential equation models, hence the need for robust numerical methods to determine their meaningful approximations. As stated in [19,20,26], certain classical numerical methods, such as Euler and Runge–Kutta, fail to properly approximate the solutions of these models, producing spurious, negative, or chaotic solutions. To avoid these uncertainties, we propose a nonstandard finite difference (NSFD) scheme for the continuous model, a technique introduced by Mickens [47,48] and further elaborated by Anguelov and Lubuma [3,4]. For the discretization of the delay part, we employ the method of Langrange interpolation proposed in [25]. Furthermore, the NSFD scheme can be used to handle the optimal control appropriately, due to its dynamical robustness. Note that the findings in Anguelov *et al.* [2] and Dimitrov *et al.* [18] support the idea that NSFD schemes are generally appropriate to solve ecological models and that in Dufourd and Dumont [19], Dumont and Tchuenche [20], NSFD schemes have been specifically developed to assess the success of mosquito control techniques.

Our discrete model is shown to be dynamically consistent in terms of existence and local stability of equilibria with the continuous delay model. Also, the positivity of solutions is preserved at all times, which fulfills a basic requirement when modeling any biological processes in general and the optimal strategies for controlling the spread of mosquitoes in particular. The trajectories of the approximate solutions are shown to approach the respective steady states regardless of the step size taken, which is never guaranteed when dealing with other numerical schemes.

The remaining part of the paper is organized as follows. Section 2 presents the biological assumptions which lead to the formulation of the mathematical model under consideration. Section 3 is concerned with the dynamics of the simplified model, completely characterizing the existence of the positive equilibrium or equilibria in terms of threshold parameters. Sufficient conditions for the stability of the trivial equilibrium and of the positive equilibrium or equilibria are also established, as well as the possible existence of stability switches and the occurrence of Hopf bifurcations. The corresponding NSFD scheme and the dynamics of the associated discrete model are investigated in Section 4, together with the consistency of the discrete model with the continuous model and its transformation into a delay-free model by the method of augmented states. The optimal control approach is addressed in Section 5, while numerical experiments, using variable environmental temperatures and meaningful ranges for the biological parameters involved, are considered in Section 6 to find the highest impact upon the size of the mosquito population. Finally, certain biologically meaningful conclusions are drawn in Section 7 on the basis of the theoretical and numerical frameworks developed in the previous sections.

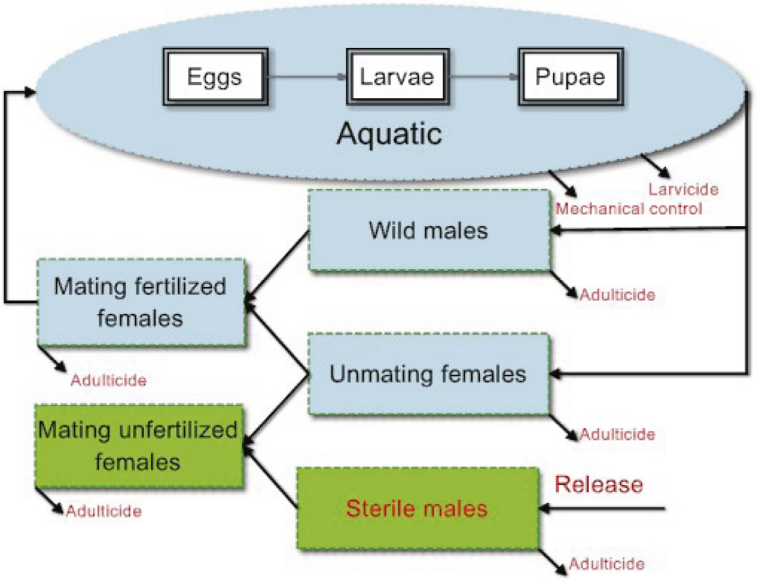

Fig. 1. The biological cycle of *Aedes aegypti* and the control mechanisms.

2. Modeling considerations

2.1. *The life cycle and control mechanisms of* Aedes aegypti

First and foremost, in order to formulate our compartmental model, it is necessary to have a basic understanding of the life cycle of a mosquito, which is divided into four stages: egg, larva, pupa, and adult or imago.

Since, for most species, adult females lay their eggs in stagnant water, we consider two main phases in our model, namely the aquatic phase (encompassing the egg, larva and pupa stages) and the adult phase. Let us denote by $A = A(t)$ the population size of the aquatic phase of the *Aedes aegypti* mosquito at time t. For the adult phase, we consider the following compartments: Y, the wild young females before mating, M, the wild males and F, the mating fertilized females. The mating fertilized females are able to lay their eggs in stagnant water on their own. The eggs are resistant to drying and hatch usually within 2–3 days, although hatching may take up to 2–3 weeks in colder climates.

The use of pesticides, including adulticide or/and larvicide treatments, is an effective way to control the spread of mosquitoes in both their larval and adult stages. Pesticide use, however, should be complemented by the use of mechanical controls in affected areas, by public health officials and residents alike, one of the essential measures being to remove stagnant water from domestic recipients, eliminating possible breeding sites.

Since the mating of sterile males with wild young females causes the mating unfertilized females U to lay unhatched eggs, we release sterile males S into the wild, with the aim of reducing the size of mosquito population by means of interfering with egg hatching. The biological cycle of *Aedes aegypti*, as modified by the control mechanisms described above, is illustrated in Fig. 1.

2.2. *Model parameters and control variables*

It is obvious that neither do all eggs hatch to larvae, nor do they all produce female mosquitoes [65]. For this reason, we denote the fraction of eggs hatching to larvae with k, $0 < k < 1$, and the fraction of female mosquitoes hatched from all eggs with f, $0 < f < 1$. Since we assume that no sex differentiation occurs in the aquatic phase, mosquitoes, after emergence from the aquatic phase to the adult phase, with survival rate η_A depending upon the ambiental temperature, as reported by [43] (see Fig. 2), are distributed between the immature female and male compartments, with ratio $\frac{1-\gamma}{\gamma}$ of male to female mosquitoes.

The flows from the compartment Y to the compartments F and U are determined by the encounters of females with wild and sterile males, respectively, and by the corresponding mating rates. Here, the terms $\frac{M}{M+S}$ and $\frac{S}{M+S}$ represent the probabilities of a random encounter of a female with a wild male and with a sterile male, respectively, and β is the mating rate of mosquitoes.

Subsequently, we assume that $(1 - \frac{\alpha}{\omega})K$ is the (controlled) capacity of aquatic forms in the breeding sites, in which α describes the action of the mechanical control and ω is a rescaling constant, $\alpha < \omega$. Since a rainy period can lead to the creation of new breeding sites and to an increase in the capacity of the existing ones, while, conversely, a dry period can reduce both the number of breeding sites and their capacity, we assume that the capacity of breeding sites also varies with the temperature.

In this regard, we assume that the capacity of breeding sites is maximal, $K = K_{\max}$, at 26.6 °C, which is the mean temperature with the maximal average amount of precipitations in northern Queensland at coastal Townsville in 1989 (see Fig. 3). We also

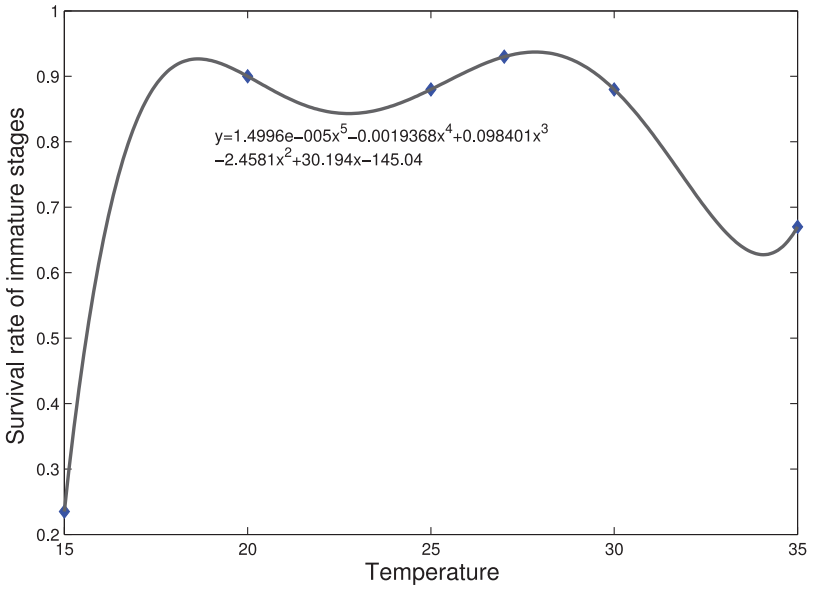

Fig. 2. The fittings of the survival rate of the immature stages as function of temperature. Fittings for the fifth degree polynomials and the observed values reported by [43] are also shown.

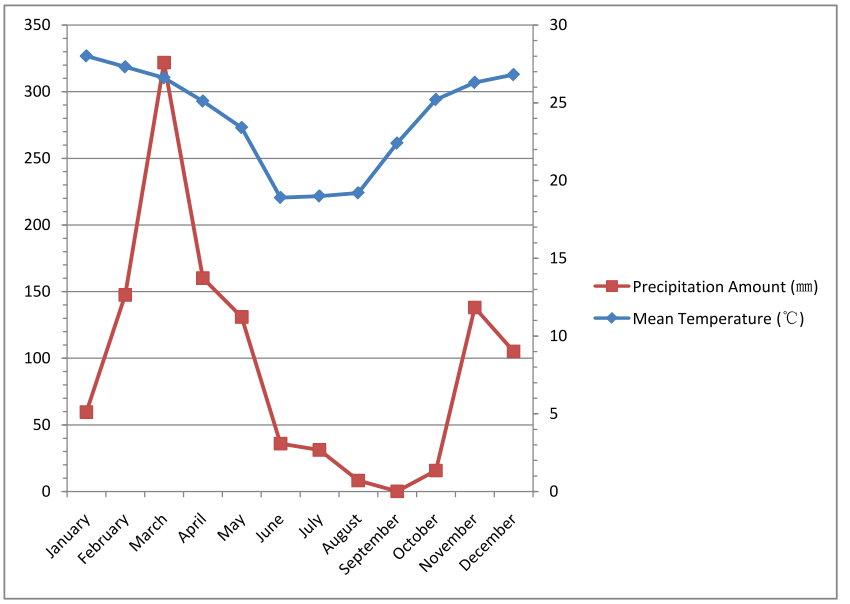

Fig. 3. Monthly mean temperature and amount of precipitation in Townsville Amo in 1989. Data reported by the weather station 942940 (YBTL), Latitude: −19.25, Longitude: 146.75, Altitude: 6.

assume that 15 °C corresponds to the austral winter, when precipitations are low and the capacity is at its lowest, $K = K_{\min}$, and that the quantitative relationship between the minimal and maximal capacities is given by $K_{\min} = 0.1 \times K_{\max}$. We may also suppose that K increases for temperatures between 15 °C and 26.6 °C. When the temperature is above 26.6 °C, we assume that K decreases due to evaporation and to a lower amount of precipitations, a concrete estimation being $K = 0.3 \times K_{\max}$ at 35 °C. Using a quadratic interpolation, we obtain a continuous relation between the carrying capacity K and the temperature (see Fig. 4).

Fig. 5 shows that the oviposition rate φ has an (approximately) linear increase with the temperature, showing indirectly that the physiological activities increase in order to maturate fertilized eggs. Since the first three aquatic stages typically last several days or even several weeks, depending on the temperature of the ambient, we assume that mosquitoes reside in compartment A τ units of time (see Fig. 5). Then the surviving individuals entering the respective compartments Y and M at time t are consequently among those that entered the aquatic phase τ units of time before. The coefficients μ_A, μ_Y, μ_M, μ_F, μ_U and μ_S represent the per capita natural mortality rates of the aquatic phase, unmating females, wild males, mating fertilized females, mating unfertilized

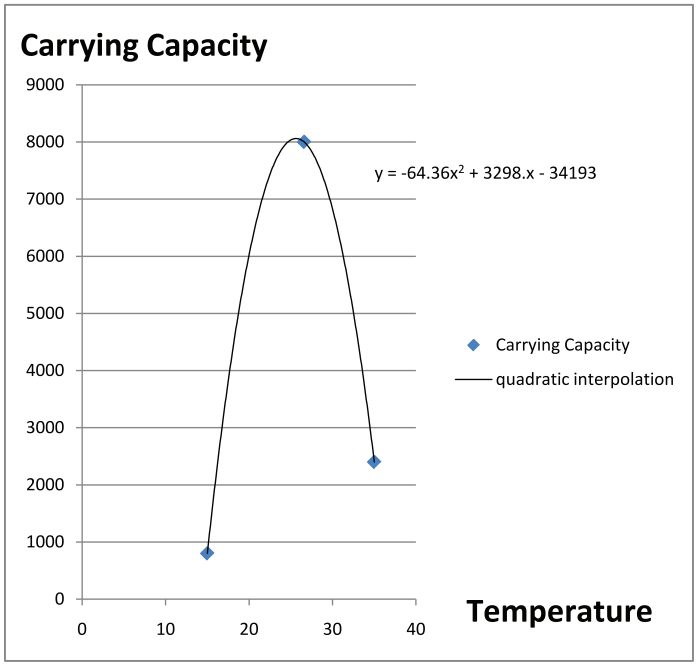

Fig. 4. The quadratic interpolation of the carrying capacity K as a function of temperature. .

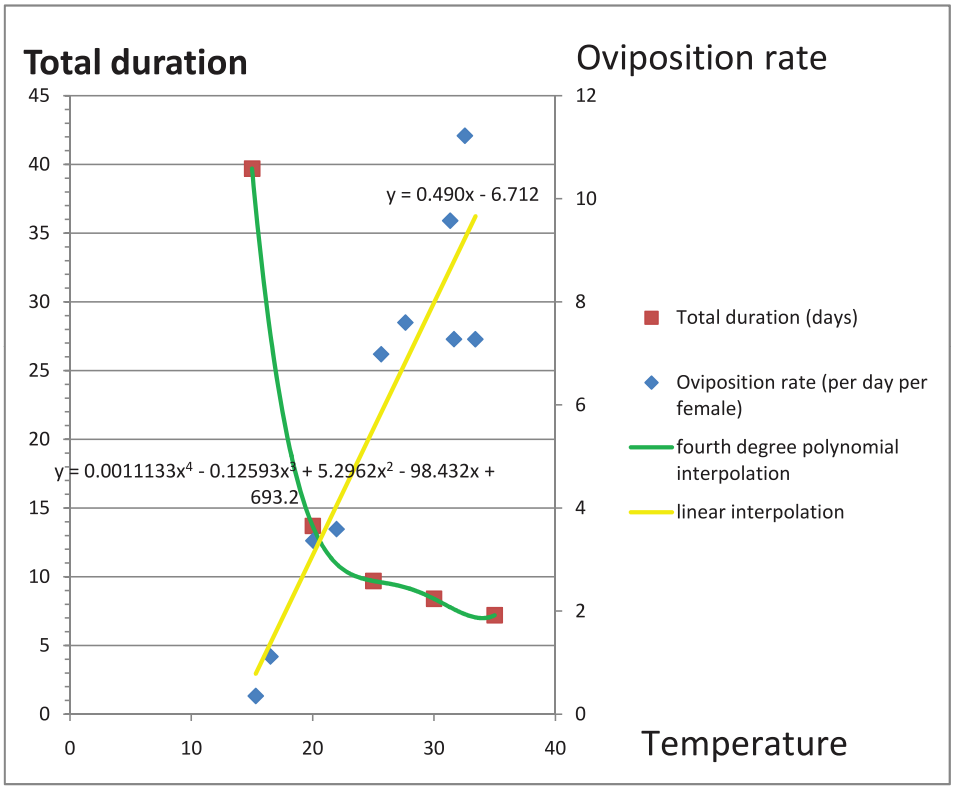

Fig. 5. Mean instar duration τ (days) and oviposition rate φ of immature stages of *Aedes aegypti* reared at different temperatures in the laboratory. The fitting of the aquatic phase oviposition rate as a function of temperature (the yellow line represents a linear interpolation). The fitting of the mean instar duration as a function of temperature (the green curve represents a fourth degree polynomial interpolation). Data reported by [43,65]. (For interpretation of the reference to color in this figure legend, the reader is referred to the web version of this article.)

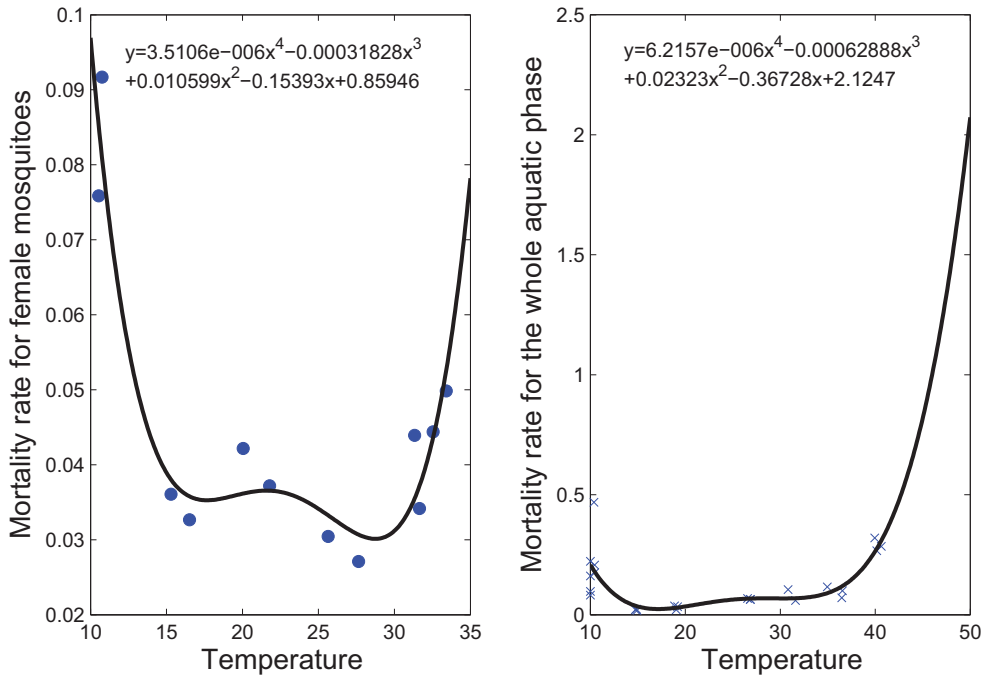

Fig. 6. The fittings of the mortality rates of the female mosquito population and, respectively, the whole aquatic phase as functions of temperature. Fittings for the fourth degree polynomials and the observed values reported by [65] are also shown.

females and sterile male mosquitoes, respectively. We fit the mortality rates of the whole aquatic phase and female mosquitoes, respectively, according to the data reported in [65] (see Fig. 6). In addition, the impacts of larvicide and adulticide upon the mosquito population can be quantified as $c_A = 1 - k_A$ and $c_M = 1 - k_M$, respectively, in which

$$k_A(t) = \exp\left(-\gamma_A i(t) + \delta_A\right)$$

and

$$k_M(t) = \exp\left(-\gamma_M i(t) + \delta_M\right).$$

Here, γ_A and γ_M are the mortality parameters of the aquatic and adult stages, respectively. The pesticide dosage function $i(t)(>0)$ is a control variable. In addition, δ_A and δ_M are the positive decay parameters for the aquatic and adult stages, respectively. From a biological viewpoint, we assume that the larvicide and adulticide degradation and natural clearance in the environment are not as rapid as to make the death rates c_A and c_M negative.

Finally, sterile insects are released at a rate $\psi(t)$. Since sterile male mosquitoes are released by humans, the positive, continuous and bounded function $\psi(t)$, understood as a control variable, describes the human intervention mechanisms, while the parameter κ can be thought as the effective mating competitiveness of the sterile males which are released and then join the wild male population to wait for mating opportunities.

2.3. The model

We now introduce our delayed model with temperature-dependent parameters in the following form

$$\frac{dA}{dt} = kf\varphi(T)\left(1 - \frac{A}{(1-\frac{\alpha}{\omega})K(T)}\right)F - (\mu_A + c_A)A - \eta_A A(t - \tau(T)), \tag{1}$$

$$\frac{dY}{dt} = \gamma\eta_A A(t - \tau(T)) - \beta Y - (\mu_Y + c_M)Y, \tag{2}$$

$$\frac{dM}{dt} = (1-\gamma)\eta_A A(t - \tau(T)) - (\mu_M + c_M)M, \tag{3}$$

$$\frac{dF}{dt} = \frac{\beta MY}{M+S} - (\mu_F + c_M)F, \tag{4}$$

$$\frac{dU}{dt} = \frac{\beta SY}{M+S} - (\mu_U + c_M)U, \tag{5}$$

$$\frac{dS}{dt} = \kappa\psi(t) - (\mu_S + c_M)S, \tag{6}$$

in which $\varphi(T)$, $K(T)$ and $\tau(T)$ are all temperature-dependent parameters. All other variables and parameters are listed in Table 2, together with their default values.

From a conceptual viewpoint, our model is related to (the SIT part of) those proposed by Dufourd and Dumont [19] and Dumont and Tchuenche [20], and is inspired by them, while keeping track of the influence of the delay and of the mating unfertilized female class U. Also, the larvicide, adulticide and mechanical controls have been first studied in Dumont and Chiroleu [21] and more recently in Liu and Stechlinski [45].

Here, for $\sigma \geq 0$ and $A \geq 0$, a function $X = (A, Y, M, F, U, S)$ is called a solution of (1)–(6) on $[\sigma - \tau(T), \sigma + A)$ if $X \in \mathbb{C}([\sigma - \tau(T), \sigma + A], \mathbb{R}^6_+)$, $(t, X_t) \in \Omega \subset \mathbb{R} \times \mathbb{C}([-\tau(T), 0], \mathbb{R}^6_+)$ and $X_t(\theta) = X(t+\theta)$ (where $\theta \in [-\tau(T), 0]$) satisfies (1)–(6) for $t \in (\sigma, \sigma + A)$. The existence and uniqueness of the solutions follow from standard results in the theory of delay differential equations [34,35,40].

Let us denote

$$\psi_{\max} = \sup_{t\in[0,\infty)} \psi(t),$$
$$\mu_{\min} = \min\{\mu_A + c_A, \mu_Y + c_M, \mu_M + c_M, \mu_F + c_M, \mu_U + c_M, \mu_S + c_M\},$$
$$B = \frac{\eta_A\left(1 - \frac{\alpha}{\omega}\right)K(T) + \kappa\psi_{\max}}{\mu_{\min}}.$$

We shall now establish the existence of a feasible region for (1)–(6).

Theorem 2.1. *The set*

$$\Gamma = \left\{(A, Y, M, F, U, S) \in \mathbb{R}^6_+ : A \leq \left(1 - \frac{\alpha}{\omega}\right)K(T); \quad Y + M + F + U + S \leq B\right\}$$

contains a feasible region for (1)–(6).

Proof. Assuming that a solution $((A, Y, M, F, U, S)$ starting inside of Γ preserves its positivity, let us observe that, from (1), $\frac{dA}{dt} \leq 0$ whenever $A \geq \left(1 - \frac{\alpha}{\omega}\right)K(T)$, which ensures the boundedness of A.

Let us also denote

$$N_A = Y + M + F + U + S.$$

Adding Eqs. (2)–(6), we see that

$$\frac{dN_A}{dt} \leq \eta_A\left(1 - \frac{\alpha}{\omega}\right)K(T) + \kappa\psi_{\max} - \mu_{\min}N_A$$

for any solution of (1)–(6) starting in Γ. By the comparison lemma, this leads to

$$N_A \leq B - (B - N(0))e^{-\mu_{\min}t},$$

which finishes the proof. □

We have not been to able prove that all solutions starting in Γ are positivity-preserving, since the system (1)–(6) is not of Kolmogorov type. However, the numerical evidence suggests that the positivity of solutions is indeed preserved for a large span of initial data.

3. The dynamics of the simplified model

3.1. The simplified model

In order to fully characterize the dynamical behavior of the solutions, we need further knowledge about the control mechanisms and temperature-dependent coefficients. In what follows, we consider fixed values for the control variables, that is, $\alpha(t) \equiv \alpha$, $\psi(t) = \psi$ and $i(t) \equiv i$, and fixed temperature of the ambient, such that φ, K and τ are also constants. Since the size of the sterile class S is controlled by human intervention and

$$\lim_{t\to+\infty} S(t) = \frac{\kappa\psi}{\mu_S + c_M},$$

for sufficiently large values of t, (1)–(6) can be simplified to the autonomous form below

$$\frac{dA}{dt} = kf\varphi\left(1 - \frac{A}{(1-\frac{\alpha}{\omega})K}\right)F - (\mu_A + c_A)A - \eta_A A(t-\tau), \tag{7}$$

$$\frac{dY}{dt} = \gamma\eta_A A(t-\tau) - \beta Y - (\mu_Y + c_M)Y, \tag{8}$$

$$\frac{dM}{dt} = (1-\gamma)\eta_A A(t-\tau) - (\mu_M + c_M)M, \tag{9}$$

$$\frac{dF}{dt} = \frac{\beta MY}{M + \frac{\kappa\psi}{\mu_S + c_M}} - (\mu_F + c_M)F, \tag{10}$$

$$\frac{dU}{dt} = \frac{\beta\frac{\kappa\psi}{\mu_S + c_M}Y}{M + \frac{\kappa\psi}{\mu_S + c_M}} - (\mu_U + c_M)U. \tag{11}$$

3.2. The existence of the equilibria

Excluding the effect of the sterile male mosquitoes from the model (1)–(6), which implies that the unfertilized class U disappears here as well, this model becomes

$$\begin{aligned}
\frac{dA}{dt} &= kf\varphi\left(1 - \frac{A}{(1-\frac{\alpha}{\omega})K}\right)F - (\mu_A + c_A)A - \eta_A A(t-\tau),\\
\frac{dY}{dt} &= \gamma\eta_A A(t-\tau) - \beta Y - (\mu_Y + c_M)Y,\\
\frac{dM}{dt} &= (1-\gamma)\eta_A A(t-\tau) - (\mu_M + c_M)M,\\
\frac{dF}{dt} &= \beta Y - (\mu_F + c_M)F.
\end{aligned}$$

It is seen by direct computations that this reduced model has a unique nontrivial equilibrium if and only if the basic offspring number

$$\mathcal{R} \doteq \frac{kf\varphi\eta_A\gamma\beta}{(\mu_F + c_M)(\mu_A + c_A + \eta_A)(\beta + \mu_Y + c_M)} > 1. \tag{12}$$

In this case, its equilibrium $X_E = (A_E, Y_E, M_E, F_E)$ has coordinates

$$\begin{aligned}
A_E &= K\left(1 - \frac{\alpha}{\omega}\right)\left(1 - \frac{1}{\mathcal{R}}\right)\\
Y_E &= \frac{\gamma\eta_A}{\beta + \mu_Y + c_M}K\left(1 - \frac{\alpha}{\omega}\right)\left(1 - \frac{1}{\mathcal{R}}\right)\\
M_E &= \frac{(1-\gamma)\eta_A}{\mu_M + c_M}K\left(1 - \frac{\alpha}{\omega}\right)\left(1 - \frac{1}{\mathcal{R}}\right)\\
F_E &= \frac{\beta}{\mu_F + c_M}\frac{\gamma\eta_A}{\beta + \mu_Y + c_M}K\left(1 - \frac{\alpha}{\omega}\right)\left(1 - \frac{1}{\mathcal{R}}\right).
\end{aligned}$$

We now determine the equilibria of the system (7)–(11), which depend on the threshold quantity $\mathcal{R}$. First of all, it can be seen that the system (7)–(11) has the trivial equilibrium $\mathbf{0} = (0, 0, 0, 0, 0)$, which represents the ideal outcome, a constant population of sterile insects.

Furthermore, we obtain a non-trivial steady state of (7)–(11) given by

$$\overline{\boldsymbol{X}} = \left(\overline{A}, \overline{Y}, \overline{M}, \overline{F}, \overline{U}\right)$$

which satisfies the following relations:

Table 1
The distribution of the roots of (14) with respect to the values of $\mathcal{R}$.

$\mathcal{R}$	Δ	Sum	Roots
$(0, \mathcal{R}_1^*)$	+	–	Two distinct negative roots
$\mathcal{R}_1^*$	0	–	A double negative root
$(\mathcal{R}_1^*, \mathcal{R}_2^*)$	–	+/0/–	Two distinct complex roots
$\mathcal{R}_2^*$	0	+	A double positive root
$(\mathcal{R}_2^*, +\infty)$	+	+	Two distinct positive roots

$$\begin{aligned}
\overline{Y} &= \frac{\gamma\eta_A}{\beta+\mu_Y+c_M}\overline{A},\\
\overline{M} &= \frac{(1-\gamma)\eta_A}{\mu_M+c_M}\overline{A},\\
\overline{F} &= \frac{\beta}{\mu_F+c_M}\frac{\overline{M}}{\overline{M}+\frac{\kappa\psi}{\mu_S+c_M}}\overline{Y},\\
\overline{U} &= \frac{\beta\frac{\kappa\psi}{\mu_S+c_M}}{(\mu_U+c_M)(\overline{M}+\frac{\kappa\psi}{\mu_S+c_M})}\overline{Y},
\end{aligned} \tag{13}$$

where $\overline{A}$ is the solution of the following algebraic equation

$$\mathcal{R}A^2 - P(\mathcal{R}-1)A + PQ = 0, \tag{14}$$

with $P = (1-\frac{\alpha}{\omega})K$ and $Q = \frac{\kappa\psi(\mu_M+c_M)}{(\mu_S+c_M)\eta_A(1-\gamma)}$.

Let us now state several properties of the second degree equation (14). The product of its roots is $\frac{PQ}{\mathcal{R}} > 0$, while their sum is $S = \frac{P(\mathcal{R}-1)}{\mathcal{R}}$. Also, its discriminant is

$$\Delta = P^2\mathcal{R}^2 - 2P(P+2Q)\mathcal{R} + P^2,$$

of second degree as a function of $\mathcal{R}$. The roots of the equation $\Delta = 0$ are

$$\mathcal{R}_1^* = \left(\sqrt{1+\frac{Q}{P}} - \sqrt{\frac{Q}{P}}\right)^2, \quad \mathcal{R}_2^* = \left(\sqrt{1+\frac{Q}{P}} + \sqrt{\frac{Q}{P}}\right)^2.$$

It is easy to verify that $0 < \mathcal{R}_1^* < 1$ and $\mathcal{R}_2^* > 1$. The distribution of the roots of (14) with respect to the values of $\mathcal{R}$ is then summarized in Table 1. Subsequently, the following result characterizes the distribution of possible equilibria of (7)–(11) with respect to the values of $\mathcal{R}$, given the fact that the trivial equilibrium $\mathbf{0}$ always exists.

Theorem 3.1. *The system (7)–(11) has*

(a) *only the trivial equilibrium* $\mathbf{0}$, *if* $\mathcal{R} \in (0, \mathcal{R}_2^*)$.
(b) *two equilibria, namely the trivial equilibrium* $\mathbf{0}$ *and a positive equilibrium* $\mathbf{X}^*$, *if* $\mathcal{R} = \mathcal{R}_2^*$.
(c) *three equilibria, namely the trivial equilibrium* $\mathbf{0}$ *and two positive equilibria* $\mathbf{X}_1^*$ *and* $\mathbf{X}_2^*$, *if* $\mathcal{R} \in (\mathcal{R}_2^*, +\infty)$.

Remark 3.2. Since the oviposition rate and the carrying capacity of the aquatic stage depend on the ambient temperature, Fig. 7 shows the impact of the environmental temperature on the existence of the equilibrium.

3.3. Stability results

The local stability of each equilibrium point is governed by the roots of the corresponding characteristic equation for the system (7)–(11). Linearizing the system (7)–(11) at an equilibrium point $\widetilde{\boldsymbol{X}}$, trivial or nontrivial,

$$\widetilde{\boldsymbol{X}} = \left(\widetilde{A}, \widetilde{Y}, \widetilde{M}, \widetilde{F}, \widetilde{U}\right),$$

we find that the corresponding characteristic polynomial is given by

$$\mathcal{P}(s) = (s+\mu_U+c_M)\mathcal{D}, \tag{15}$$

where

$$\mathcal{D} = \det\begin{pmatrix}
s+\frac{kf\varphi}{P}\widetilde{F}+\mu_A+c_A+\eta_A e^{-s\tau} & 0 & 0 & -kf\varphi(1-\frac{\widetilde{A}}{P})\\
-\gamma\eta_A e^{-s\tau} & s+\beta+\mu_Y+c_M & 0 & 0\\
-(1-\gamma)\eta_A e^{-s\tau} & 0 & s+\mu_M+c_M & 0\\
0 & -\frac{\beta\widetilde{M}}{\widetilde{M}+\frac{\kappa\psi}{\mu_S+c_M}} & -\frac{\beta\frac{\kappa\psi}{\mu_S+c_M}\widetilde{Y}}{(\widetilde{M}+\frac{\kappa\psi}{\mu_S+c_M})^2} & s+\mu_F+c_M
\end{pmatrix}$$

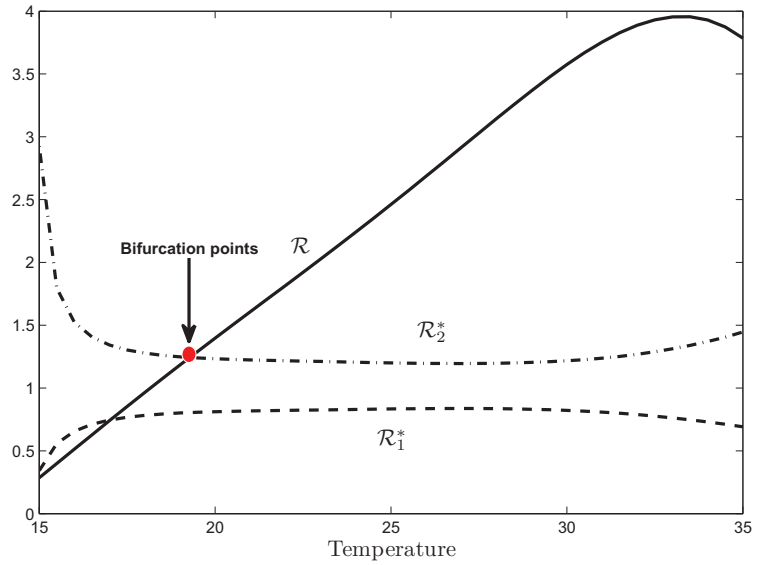

Fig. 7. Impact of the environmental temperature on the existence of the equilibria. Here, $k = f = 0.9$, $\psi \equiv 40$, $\kappa = 0.6$, $i \equiv 0.4$, $\alpha \equiv 0.4$, the other parameters being given in Table 2.

Let us start with the stability of the trivial equilibrium $\mathbf{0} = (0, 0, 0, 0, 0)$. It is seen that the eigenvalues of the corresponding Jacobian matrix are $-(\beta + \mu_Y + c_M)$, $-(\mu_M + c_M)$, $-(\mu_F + c_M)$, $-(\mu_U + c_M)$ and the solutions of the following transcendental equation

$$s + \mu_A + c_A + \eta_A e^{-s\tau} = 0. \tag{16}$$

In view of Theorem 3.1, together with Theorem 2.1 in Chapter 3 of [40], we obtain the following result, which characterizes the stability switches of the trivial equilibrium.

Theorem 3.3. *The following statements hold.*

(i) *If $\eta_A \le \mu_A + c_A$, then the trivial equilibrium $\mathbf{0}$ is locally asymptotically stable for any positive delay τ.*
(ii) *If $\eta_A > \mu_A + c_A$, then the trivial equilibrium $\mathbf{0}$ is locally asymptotically stable when $\tau < \tau^*$ and unstable when $\tau > \tau^*$, where*

$$\tau^* \doteq \frac{\operatorname{arccot}\left(-\frac{\mu_A + c_A}{\sqrt{\eta_A^2 - (\mu_A + c_A)^2}}\right)}{\sqrt{\eta_A^2 - (\mu_A + c_A)^2}}.$$

We now consider the stability of the positive equilibria.

When $\mathcal{R} \in (\mathcal{R}_2^*, +\infty)$, it is seen that $P(\mathcal{R} - 1) > 2\sqrt{PQ\mathcal{R}}$ and the system (7)–(11) has two positive equilibria

$$\boldsymbol{X}_1^* = (A_1^*, Y_1^*, M_1^*, F_1^*, U_1) \quad \text{and } \boldsymbol{X}_2^* = (A_2^*, Y_2^*, M_2^*, F_2^*, U_2^*),$$

in which

$$A_1^* = \frac{P(\mathcal{R} - 1) - \sqrt{(P(\mathcal{R} - 1))^2 - 4\mathcal{R}PQ}}{2\mathcal{R}}, \quad A_2^* = \frac{P(\mathcal{R} - 1) + \sqrt{(P(\mathcal{R} - 1))^2 - 4\mathcal{R}PQ}}{2\mathcal{R}},$$

and Y_l^*, M_l^*, F_l^* and $U_l^* (l = 1, 2)$ satisfy the relations (13). It follows that

$$A_1^* = \frac{2PQ}{P(\mathcal{R} - 1) + \sqrt{(P(\mathcal{R} - 1))^2 - 4\mathcal{R}PQ}} < \sqrt{\frac{PQ}{\mathcal{R}}}, \quad A_2^* > \sqrt{\frac{PQ}{\mathcal{R}}}. \tag{17}$$

In view of (15), we obtain that the corresponding characteristic polynomial at $\boldsymbol{X}_l^*$, $(l = 1, 2)$ is given by

$$\mathcal{P}(s)|_{\boldsymbol{X}_l^*} = (s + \mu_U + c_M)\left(\left(s + \frac{kf\varphi}{P}F_l^* + \mu_A + c_A + \eta_A e^{-s\tau}\right)\right.$$
$$\left. \times \det\begin{pmatrix} s + \beta + \mu_Y + c_M & 0 & 0 \\ 0 & s + \mu_M + c_M & 0 \\ -\frac{\beta M_l^*}{M_l^* + \frac{\kappa\psi}{\mu_S + c_M}} & -\frac{\beta \frac{\kappa\psi}{\mu_S + c_M} Y_l^*}{(M_l^* + \frac{\kappa\psi}{\mu_S + c_M})^2} & s + \mu_F + c_M \end{pmatrix} + kf\varphi\left(1 - \frac{A_l^*}{P}\right)\right)$$

$$\times \det\left(\begin{array}{ccc} -\gamma\eta_A e^{-s\tau} & s+\beta+\mu_Y+c_M & 0 \\ -(1-\gamma)\eta_A e^{-s\tau} & 0 & s+\mu_M+c_M \\ 0 & -\frac{\beta M_l^*}{M_l^*+\frac{\kappa\psi}{\mu_S+c_M}} & -\frac{\beta\frac{\kappa\psi}{\mu_S+c_M}Y_l^*}{(M_l^*+\frac{\kappa\psi}{\mu_S+c_M})^2} \end{array}\right)\Bigg)\Bigg).$$

$$= (s+\mu_U+c_M)\Big(\varrho_{1l}(s)+\big(\varrho_{2l}(s)-\varrho_{3l}(s)\big)e^{-s\tau}\Big),$$

in which

$$\varrho_{1l}(s) = \left(s+\frac{\mathcal{R}(\mu_A+c_A+\eta_A)(A_l^*)^2}{P(A_l^*+Q)}+\mu_A+c_A\right)(s+\beta+\mu_Y+c_M)(s+\mu_M+c_M)(s+\mu_F+c_M),$$

$$\varrho_{2l}(s) = \eta_A(s+\beta+\mu_Y+c_M)(s+\mu_M+c_M)(s+\mu_F+c_M)$$

$$\varrho_{3l}(s) = kf\varphi\gamma\eta_A\beta\left(1-\frac{A_l^*}{P}\right)\left[\frac{A_l^*}{A_l^*+Q}(s+\mu_M+c_M)+\frac{Q(\mu_M+c_M)A_l^*}{(\beta+\mu_Y+c_M)(A_l^*+Q)^2}(s+\beta+\mu_Y+c_M)\right].$$

Let us observe that, for $l=1,2$, ϱ_{1l} and $\varrho_{2l}-\varrho_{3l}$ are polynomials with real coefficients, of degree 4 and 3, respectively, which do not have common imaginary roots since all roots of ϱ_{1l} are real. It is seen that

$$\varrho_{1l}(0) = \left(\frac{\mathcal{R}(\mu_A+c_A+\eta_A)(A_l^*)^2}{P(A_l^*+Q)}+\mu_A+c_A\right)(\beta+\mu_Y+c_M)(\mu_M+c_M)(\mu_F+c_M)$$

$$>0$$

$$\varrho_{2l}(0)-\varrho_{3l}(0) = (\beta+\mu_Y+c_M)(\mu_M+c_M)(\mu_F+c_M)\left[\eta_A-(\mu_A+c_A+\eta_A)\left(1+\frac{Q}{A_l^*+Q}\right)\right]<0$$

$$\varrho_{1l}(0)+\varrho_{2l}(0)-\varrho_{3l}(0) = (\beta+\mu_Y+c_M)(\mu_M+c_M)(\mu_F+c_M)(\mu_A+c_A+\eta_A)\frac{1}{P(A_l^*+Q)}\left[\mathcal{R}(A_l^*)^2-PQ\right].$$

By (17), it follows that

$$\varrho_{11}(0)+\varrho_{21}(0)-\varrho_{31}(0)<0$$
$$\varrho_{12}(0)+\varrho_{22}(0)-\varrho_{32}(0)>0.$$

Let us also denote

$$F_l(s) = |\varrho_{1l}(is)|^2-|\varrho_{2l}(is)-\varrho_{3l}(is)|^2, \quad l=1,2, \quad i \text{ is the imaginary unit}$$

and observe that F_1, F_2 are polynomials of order 8 with positive leading coefficients such that

$$F_1(0)<0, \quad F_2(0)>0.$$

Consequently, the equation $F_1(s)=0$ has at least a positive solution, while the equation $F_2(s)=0$ may or may not have any. By Theorem 1 in [14], one then obtains the following stability result.

Theorem 3.4. *The following statements hold.*

(i) *If the positive roots of equation $F_1(s)=0$ are all simple, then as τ increases, a finite number of stability switches occur and there exists a positive number τ_1^* such that $\boldsymbol{X}_1^*$ is unstable for any delay $\tau>\tau_1^*$.*

(ii) *If the equation $F_2(s)=0$ has no positive roots, then $\boldsymbol{X}_2^*$ is stable for any positive delay τ. If the equation $F_2(s)=0$ has at least a positive root and all positive roots are simple, then as τ increases, a finite number of stability switches occur and there exists a positive number τ_2^* such that $\boldsymbol{X}_2^*$ is unstable for any delay $\tau>\tau_2^*$.*

Since F_2 is a polynomial of degree 8, the conditions to ensure that the equation $F_2(s)=0$ has no positive roots have mostly a theoretical relevance, though. However, another contribution of Theorem 3.4 is that $\boldsymbol{X}_2^*$, the equilibrium with more mosquitoes in the aquatic phase, has more chances to be stable, confirming the idea that "rich" equilibria are prone to stability. See [27] for a related result describing the dynamics of a predator-prey model with stage structure. Note that if $\mathcal{R}=\mathcal{R}_2^*$, one has

$$\varrho_{11}(0)+\varrho_{21}(0)-\varrho_{31}(0)=0$$
$$\varrho_{12}(0)+\varrho_{22}(0)-\varrho_{32}(0)=0,$$

and Theorem 1 in [14] is not applicable anymore. Let us consequently treat the case in which $\mathcal{R}=\mathcal{R}_2^*$ separately.

When $\mathcal{R}=\mathcal{R}_2^*$, the system (7)–(11) has the positive equilibrium

$$\boldsymbol{X}^* = (A^*, Y^*, M^*, F^*, U^*),$$

in which $A^*=\frac{P(\mathcal{R}-1)}{2\mathcal{R}}=\sqrt{\frac{PQ}{\mathcal{R}}}$ and Y^*, M^*, F^*, U^* satisfy (13). Again, in view of (15), we obtain that the corresponding characteristic polynomial at $\boldsymbol{X}^*$ is given by

$$\mathcal{P}(s)|_{\boldsymbol{X}^*} = (s+\mu_U+c_M)(\varrho_1(s)+\big(\varrho_2(s)-\varrho_3(s)\big)e^{-s\tau}), \tag{19}$$

in which

$$\varrho_1(s) = \left(s + \frac{\mathcal{R}(\mu_A + c_A + \eta_A)(A^*)^2}{P(A^* + Q)} + \mu_A + c_A\right)(s + \beta + \mu_Y + c_M)(s + \mu_M + c_M)(s + \mu_F + c_M),$$

$$\varrho_2(s) = \eta_A(s + \beta + \mu_Y + c_M)(s + \mu_M + c_M)(s + \mu_F + c_M)$$

and

$$\varrho_3(s) = kf\varphi\gamma\eta_A\beta\left(1 - \frac{A^*}{P}\right)\left(\frac{A^*}{A^* + Q}(s + \mu_M + c_M) + \frac{Q(\mu_M + c_M)A^*}{(\beta + \mu_Y + c_M)(A^* + Q)^2}(s + \beta + \mu_Y + c_M)\right).$$

Obviously, one of the eigenvalues of the corresponding Jacobian matrix is $-(\mu_U + c_M)$. In the following, let us now turn to the problem of localizing the zeroes of the function

$$h(s, e^s) = \varrho_1(s)e^{s\tau} + \varrho_2(s) - \varrho_3(s). \tag{20}$$

Let $Z = s\tau$ and define

$$H(Z) = h\left(\frac{Z}{\tau}, e^{\frac{Z}{\tau}}\right) = \varrho_1\left(\frac{Z}{\tau}\right)e^Z + \varrho_2\left(\frac{Z}{\tau}\right) - \varrho_3\left(\frac{Z}{\tau}\right).$$

Hence

$$\begin{aligned} H(iy) &= \left(\frac{y^4}{\tau^4} - \frac{a_2y^2}{\tau^2} + a_0\right)\cos y - \left(\frac{a_1y}{\tau} - \frac{a_3y^3}{\tau^3}\right)\sin y - \frac{b_2y^2}{\tau^2} + b_0 \\ &\quad + i\left[\left(\frac{y^4}{\tau^4} - \frac{a_2y^2}{\tau^2} + a_0\right)\sin y + \left(\frac{a_1y}{\tau} - \frac{a_3y^3}{\tau^3}\right)\cos y + \left(\frac{b_1y}{\tau} - \frac{b_3y^3}{\tau^3}\right)\right] \\ &\doteq \mathcal{F}_1(y; a_2, a_0)\cos y - \mathcal{F}_2(y; a_1, a_3)\sin y + \mathcal{F}_3(y; b_0, b_2) \\ &\quad + i\big(\mathcal{F}_1(y; a_2, a_0)\sin y + \mathcal{F}_2(y; a_1, a_3)\cos y + \mathcal{F}_4(y; b_1, b_3)\big), \end{aligned}$$

in which

$$\begin{aligned} a_3 &= \left(\frac{\mathcal{R}(\mu_A + c_A + \eta_A)(A^*)^2}{P(A^* + Q)} + \mu_A + c_A\right) + (\beta + \mu_Y + c_M) + (\mu_M + c_M) + (\mu_F + c_M); \\ a_2 &= \left(\frac{\mathcal{R}(\mu_A + c_A + \eta_A)(A^*)^2}{P(A^* + Q)} + \mu_A + c_A\right)\big((\beta + \mu_Y + c_M) + (\mu_M + c_M) + (\mu_F + c_M)\big) \\ &\quad + (\beta + \mu_Y + c_M)\big((\mu_M + c_M) + (\mu_F + c_M)\big) + (\mu_M + c_M)(\mu_F + c_M); \\ a_1 &= \left(\frac{\mathcal{R}(\mu_A + c_A + \eta_A)(A^*)^2}{P(A^* + Q)} + \mu_A + c_A\right)(\beta + \mu_Y + c_M)\big((\mu_M + c_M) + (\mu_F + c_M)\big) \\ &\quad + \left[\left(\frac{\mathcal{R}(\mu_A + c_A + \eta_A)(A^*)^2}{P(A^* + Q)} + \mu_A + c_A\right) + (\beta + \mu_Y + c_M)\right](\mu_M + c_M)(\mu_F + c_M); \\ a_0 &= \left(\frac{\mathcal{R}(\mu_A + c_A + \eta_A)(A^*)^2}{P(A^* + Q)} + \mu_A + c_A\right)(\beta + \mu_Y + c_M)(\mu_M + c_M)(\mu_F + c_M); \end{aligned} \tag{21}$$

$$\begin{aligned} b_3 &= \eta_A; \\ b_2 &= \eta_A\big((\beta + \mu_Y + c_M) + (\mu_M + c_M) + (\mu_F + c_M)\big); \\ b_1 &= \eta_A\big((\beta + \mu_Y + c_M)\big((\mu_M + c_M) + (\mu_F + c_M)\big) + (\mu_M + c_M)(\mu_F + c_M)\big) \\ &\quad - kf\varphi\gamma\eta_A\beta\left(1 - \frac{A^*}{P}\right)\left[\frac{A^*}{A^* + Q} + \frac{Q(\mu_M + c_M)A^*}{(\beta + \mu_Y + c_M)(A^* + Q)^2}\right]; \\ b_0 &= \eta_A(\beta + \mu_Y + c_M)(\mu_M + c_M)(\mu_F + c_M) - kf\varphi\gamma\eta_A\beta\left(1 - \frac{A^*}{P}\right) \\ &\quad \times \left[\frac{A^*}{A^* + Q}(\mu_M + c_M) + \frac{Q(\mu_M + c_M)A^*}{(\beta + \mu_Y + c_M)(A^* + Q)^2}(\beta + \mu_Y + c_M)\right]. \end{aligned}$$

To introduce our next stability result, let us mention that the zeroes of two real single-variable functions a and b are said to alternate if the functions have no common root or multiple zeroes and between two zeroes of a function there is a zero of the other. Using Theorem 13.7 in [6], we are then able to state the following result, which complements Theorem 3.4 by dealing with the limit case $\mathcal{R} = \mathcal{R}_2^*$.

Theorem 3.5. *Suppose that $\mathcal{R} = \mathcal{R}_2^*$. Then the unique positive equilibrium $\boldsymbol{X}^*$ of (7)–(11) is locally asymptotically stable if one of the following conditions is satisfied.*

(a) *All roots of the equations*

$$\mathcal{F}_1(y; a_2, a_0)\cos y - \mathcal{F}_2(y; a_1, a_3)\sin y + \mathcal{F}_3(y; b_0, b_2) = 0 \tag{22}$$

and

$$\mathcal{F}_1(y; a_2, a_0)\sin y + \mathcal{F}_2(y; a_1, a_3)\cos y + \mathcal{F}_4(y; b_1, b_3) = 0 \tag{23}$$

are real and alternate and the inequality

$$\begin{aligned}&\mathcal{F}_1^2 + \mathcal{F}_2^2 + \mathcal{F}_1\mathcal{F}_2' - \mathcal{F}_1'\mathcal{F}_2 + \mathcal{F}_3\mathcal{F}_4' - \mathcal{F}_3'\mathcal{F}_4\\ &\quad > \sin y(\mathcal{F}_1\mathcal{F}_3' - \mathcal{F}_1'\mathcal{F}_3 + \mathcal{F}_2\mathcal{F}_4' - \mathcal{F}_2'\mathcal{F}_4 + \mathcal{F}_2\mathcal{F}_3 - \mathcal{F}_1\mathcal{F}_4)\\ &\qquad + \cos y(\mathcal{F}_1'\mathcal{F}_4 - \mathcal{F}_1\mathcal{F}_4' + \mathcal{F}_2\mathcal{F}_3' - \mathcal{F}_2'\mathcal{F}_3 - \mathcal{F}_1\mathcal{F}_3 - \mathcal{F}_2\mathcal{F}_4)\end{aligned}$$

holds for at least a value of y.

(b) *All roots of (22) are real and, for each root $y = y^*$,*

$$\begin{aligned}&\big(\mathcal{F}_1'(y^*)\cos y^* - \mathcal{F}_1(y^*)\sin y^* - \mathcal{F}_2'(y^*)\sin y^* - \mathcal{F}_2(y^*)\cos y^* + \mathcal{F}_3'(y^*)\big)\\ &\quad\times\big(\mathcal{F}_1(y^*)\sin y^* + \mathcal{F}_2(y^*)\cos y^* + \mathcal{F}_4(y^*)\big) < 0.\end{aligned}$$

(c) *All the roots of (23) are real and, for each root $y = y^*$,*

$$\begin{aligned}&\big(\mathcal{F}_1'(y^*)\sin y^* + \mathcal{F}_1(y^*)\cos y^* + \mathcal{F}_2'(y^*)\cos y^* - \mathcal{F}_2(y^*)\sin y^* + \mathcal{F}_4'(y^*)\big)\\ &\quad\times\big(\mathcal{F}_1(y^*)\cos y^* - \mathcal{F}_2(y^*)\sin y^* + \mathcal{F}_3(y^*)\big) < 0.\end{aligned}$$

3.4. The existence of Hopf bifurcations

In this subsection, we shall study the occurrence of Hopf bifurcations on condition that $\mathcal{R} \geq \mathcal{R}_2^*$, which implies that there are two positive equilibria $\boldsymbol{X}_l^*$, $l = 1, 2$, which coincide when $\mathcal{R} = \mathcal{R}_2^*$.

The characteristic equation at $\boldsymbol{X}_l^*$, $l = 1, 2$, has a simple negative root $-(\mu_U + c_M)$, the remaining roots verifying the transcendental equation

$$\varrho_{1l}(s) + \big(\varrho_{2l}(s) - \varrho_{3l}(s)\big)e^{-s\tau} = 0,$$

in which ϱ_{1l}, ϱ_{2l}, ϱ_{3l} are given by (18).

For correspondence with the notations used in the previous subsection, let a_{3l}, a_{2l}, a_{1l}, a_{0l}, $l = 1, 2$, be the quantities obtained replacing A^* with A_l^* in the formulas for a_3, a_2, a_1, a_0 given by (21), respectively. Let also b_{3l}, b_{2l}, b_{1l}, b_{0l}, $l = 1, 2$, be the quantities obtained replacing A^* with A_l^* in the formulas for b_3, b_2, b_1, b_0 given by (21), respectively (actually, b_{3l} and b_{2l} do not depend upon l, but we shall keep this notation for the sake of consistency).

This leads to

$$s^4 + a_{3l}s^3 + a_{2l}s^2 + a_{1l}s + a_{0l} + (b_{3l}s^3 + b_{2l}s^2 + b_{1l}s + b_{0l})e^{-s\tau} = 0, \tag{24}$$

We now find conditions for the existence of purely imaginary roots of (24).

Lemma 3.1. *If conditions*

$$a_{3l}^2 - 2a_{2l} - b_{3l}^2 > 0, \quad a_{2l}^2 + 2a_{0l} - 2a_{3l}a_{1l} - b_{2l}^2 + 2b_{3l}b_{1l} > 0, \quad a_{0l}^2 - b_{0l}^2 < 0, \tag{25}$$

hold for an $l \in \{1, 2\}$, then Eq. (24) corresponding to that l has a unique pair of purely imaginary roots.

Proof. If $s = iw$, $w > 0$, is a root of (24), we observe that

$$w^4 - a_{3l}iw^3 - a_{2l}w^2 + a_{1l}iw + a_{0l} + (-b_{3l}iw^3 - b_{2l}w^2 + b_{1l}iw + b_{0l})(\cos w\tau - i\sin w\tau) = 0.$$

After separating real and imaginary parts, we see that

$$\begin{aligned}w^4 - a_{2l}w^2 + a_{0l} &= (b_{2l}w^2 - b_{0l})\cos w\tau + (b_{3l}w^3 - b_1w)\sin w\tau\\ -a_{3l}w^3 + a_{1l}w &= (b_{3l}w^3 - b_{1l}w)\cos w\tau - (b_{2l}w^2 - b_{0l})\sin w\tau.\end{aligned} \tag{26}$$

By squaring and adding both equations in (26), we obtain that

$$(w^4 - a_{2l}w^2 + a_{0l})^2 + (-a_{3l}w^3 + a_{1l}w)^2 = (b_{2l}w^2 - b_{0l})^2 + (b_{3l}w^3 - b_{1l}w)^2, \tag{27}$$

which leads to

$$w^8 + T_3w^6 + T_2w^4 + T_1w^2 + T_0 = 0, \tag{28}$$

with

$$T_3 = a_{3l}^2 - 2a_{2l} - b_{3l}^2$$
$$T_2 = a_{2l}^2 + 2a_{0l} - 2a_{3l}a_{1l} - b_{2l}^2 + 2b_{3l}b_{1l}$$
$$T_1 = -2a_{2l}a_{0l} + a_{1l}^2 + 2b_{2l}b_{0l} - b_{1l}^2$$
$$T_0 = a_{0l}^2 - b_{0l}^2.$$

From our hypotheses, $T_3 > 0$, $T_2 > 0$ and $T_0 < 0$. By Descartes' rule of signs, it follows that the equation

$$u^4 + T_3u^3 + T_2u^2 + T_1u + T_0 = 0$$

has exactly one positive root. In turn, this implies that there is a unique positive root w_0 of (28) and that (24) has a unique pair of purely imaginary roots $\pm iw_0$.

From (26), one may determine the corresponding values of τ. To this purpose, we denote

$$D = (w^4 - a_{2l}w^2 + a_{0l})^2 + (-a_{3l}w^3 + a_{1l}w)^2 = (b_{2l}w^2 - b_{0l})^2 + (b_{3l}w^3 - b_{1l}w)^2.$$

Since

$$\cos w\tau = \frac{1}{D}\big[(b_{2l} - b_{3l}a_{3l})w^6 + (-a_{2l}b_{2l} - b_{0l} + b_{3l}a_{1l} + b_{1l}a_{3l})w^4 + (2a_{0l}b_{2l} - b_{1l}a_{1l})w^2 - a_{0l}b_{0l}\big],$$

it follows that

$$\tau_n^1 = \frac{1}{w_0}\left\{\arccos\left(\frac{1}{D}\big[(b_{2l} - b_{3l}a_{3l})w^6 + (-a_{2l}b_{2l} - b_{0l} + b_{3l}a_{1l} + b_{1l}a_{3l})w^4 + (2a_{0l}b_{2l} - b_{1l}a_{1l})w^2 - a_{0l}b_{0l}\big]\right) + 2n\pi\right\}, \quad n \geq 0,$$

or

$$\tau_n^2 = \frac{1}{w_0}\left\{-\arccos\left(\frac{1}{D}\big[(b_{2l} - b_{3l}a_{3l})w^6 + (-a_{2l}b_{2l} - b_{0l} + b_{3l}a_{1l} + b_{1l}a_{3l})w^4 + (2a_{0l}b_{2l} - b_{1l}a_{1l})w^2 - a_{0l}b_{0l}\big]\right) + 2n\pi\right\}, \quad n \geq 1.$$

□

Having found the unique pair of purely imaginary roots $\pm iw_0$, $w_0 > 0$ for (24), we now determine sufficient hypotheses for the transversality condition to hold at iw_0.

Lemma 3.2. *Let $\pm iw_0$, $w_0 > 0$, be the unique pair of purely imaginary roots found by means of Lemma 3.1. If conditions*

$$a_{1l}^2 - 2a_{0l}a_{2l} + b_{1l}b_{3l} + 2b_{0l}b_{2l} > 0, \quad 3(2a_{2l} + b_{3l}^2)^2 - 16(a_{0l} - a_{1l}a_{3l} + b_{1l}b_{3l} - b_{2l}^2) < 0, \tag{29}$$

hold for the same l, then the transversality condition

$$\mathrm{Re}\left(\frac{ds}{d\tau}\right)^{-1}\bigg|_{s=iw_0} > 0,$$

is satisfied for that l.

Proof. By differentiating (24) with respect to τ, one obtains that

$$\big[4s^3 + 3a_{3l}s^2 + 2a_{2l}s + a_{1l} + (3b_{3l}s^2 + 2b_{2l}s + b_{1l})e^{-s\tau} - \tau(b_{3l}s^3 + b_{2l}s^2 + b_{1l}s + b_{0l})e^{-s\tau}\big]\frac{ds}{dt} = s(b_{3l}s^3 + b_{2l}s^2 + b_{1l}s + b_{0l})e^{-s\tau},$$

which yields

$$\left(\frac{ds}{d\tau}\right)^{-1} = -\frac{4s^3 + 3a_{3l}s^2 + 2a_{2l}s + a_{1l}}{s(s^4 + a_{3l}s^3 + a_{2l}s^2 + a_{1l}s + a_{0l})} + \frac{3b_{3l}s^2 + 2b_{2l}s + b_{1l}}{s(b_{3l}s^3 + b_{2l}s^2 + b_{1l}s + b_{0l})} - \frac{\tau}{s}.$$

It consequently follows that

$$\begin{aligned}\mathrm{Re}\left(\frac{ds}{d\tau}\right)^{-1}\Big|_{s=iw_0} &= \mathrm{Re}\left(-\frac{(a_{1l}-3a_{3l}w_0^2)+i(2w_0a_{2l}-4w_0^3)}{iw_0\left[(a_{0l}-a_{2l}w_0^2+w_0^4)+i(-a_{3l}w_0^3+a_{1l}w_0)\right]}\right)\\ &\quad+\mathrm{Re}\left(\frac{(b_{1l}-3b_{3l}w_0^2)+2b_{2l}w_0 i}{iw_0\left[(b_{0l}-b_{2l}w_0^2)+i(b_{1l}w_0-b_{3l}w_0^3)\right]}\right)\\ &= \frac{(a_{1l}-3a_{3l}w_0^2)(-a_{3l}w_0^3+a_{1l}w_0)-(2w_0a_{2l}-4w_0^3)(a_{0l}-a_{2l}w_0^2+w_0^4)}{w_0\left[(a_{0l}-a_{2l}w_0^2+w_0^4)^2+(-a_{3l}w_0^3+a_{1l}w_0)^2\right]}\\ &\quad+\frac{2b_{2l}w_0(b_{0l}-2b_{2l}w_0^2)-(b_{1l}-3b_{3l}w_0^2)(b_{1l}w_0-b_{3l}w_0^3)}{w_0\left[(b_{0l}-b_{2l}w_0^2)^2+(b_{1l}w_0-b_{3l}w_0^3)^2\right]}.\end{aligned}$$

This leads to

$$\begin{aligned}\mathrm{Re}\left(\frac{ds}{d\tau}\right)^{-1}\Big|_{s=iw_0} &= \frac{4w_0^6-6a_{2l}w_0^4+4(a_{0l}-a_{1l}a_{3l})w_0^2+(a_{1l}^2-2a_{0l}a_{2l})}{(w^4-a_{2l}w^2+a_{0l})^2+(-a_{3l}w^3+a_{1l}w)^2}\\ &\quad+\frac{-3b_{3l}^2w_0^4+4(b_{1l}b_{3l}-b_{2l}^2)w_0^2+(b_{1l}b_{3l}+2b_{0l}b_{2l})}{(b_{2l}w^2-b_{0l})^2+(b_{3l}w^3-b_{1l}w)^2}.\end{aligned}$$

Having in view (27), it follows that

$$\begin{aligned}\mathrm{Re}\left(\frac{ds}{d\tau}\right)^{-1}\Big|_{s=iw_0} &= \left[4w_0^6-(6a_{2l}+3b_{3l}^2)w_0^4+4(a_{0l}-a_{1l}a_{3l}+b_{1l}b_{3l}-b_{2l}^2)w_0^2\right.\\ &\quad\left.+(a_{1l}^2-2a_{0l}a_{2l}+b_{1l}b_{3l}+2b_{0l}b_{2l})\right]\cdot\frac{1}{D},\end{aligned}$$

with

$$D=(w^4-a_{2l}w^2+a_{0l})^2+(-a_{3l}w^3+a_{1l}w)^2=(b_{2l}w^2-b_{0l})^2+(b_{3l}w^3-b_{1l}w)^2.$$

Let

$$\begin{aligned}f(w) &= 4w^6-(6a_{2l}+3b_{3l}^2)w^4+4(a_{0l}-a_{1l}a_{3l}+b_{1l}b_{3l}-b_{2l}^2)w^2\\ &\quad+(a_{1l}^2-2a_{0l}a_{2l}+b_{1l}b_{3l}+2b_{0l}b_{2l})\\ F(v) &= 4v^3-(6a_{2l}+3b_{3l}^2)v^2+4(a_{0l}-a_{1l}a_{3l}+b_{1l}b_{3l}-b_{2l}^2)v\\ &\quad+(a_{1l}^2-2a_{0l}a_{2l}+b_{1l}b_{3l}+2b_{0l}b_{2l}).\end{aligned}$$

Then

$$F'(v)=12v^2-6(2a_{2l}+b_{3l}^2)v+4(a_{0l}-a_{1l}a_{3l}+b_{1l}b_{3l}-b_{2l}^2).$$

Assume that

$$3(2a_{2l}+b_{3l}^2)^2-16(a_{0l}-a_{1l}a_{3l}+b_{1l}b_{3l}-b_{2l}^2)<0.$$

Then the quadratic equation $F'(v)=0$ has no real roots (note that if it has, then at least one of the roots is positive, since their sum is $\frac{1}{2}(2a_{2l}+b_{3l}^2)$). It then follows that F is monotonically increasing on $\mathbb{R}$, and consequently f is monotonically increasing on $[0,\infty)$. Since

$$f(0)=a_{1l}^2-2a_{0l}a_{2l}+b_{1l}b_{3l}+2b_{0l}b_{2l}>0,$$

it follows that f is strictly positive on $[0,\infty)$ and consequently,

$$\mathrm{Re}\left(\frac{ds}{d\tau}\right)^{-1}\Big|_{s=iw_0}>0,$$

that is, the transversality condition holds at $s=iw_0$. □

By combining Lemmas 3.1 and 3.2 and using Hopf's bifurcation theorem (see Guckenheimer and Holmes [32], Theorem 3.4.2), one may obtain the following result.

Theorem 3.6. *If conditions (25) and (29) hold for an $l\in\{1,2\}$, then the system (7)–(11) undergoes a Hopf bifurcation at $\boldsymbol{X}_l^*$, when $\tau=\tau_n^1$, $n\geq 0$, or $\tau=\tau_n^2$, $n\geq 1$.*

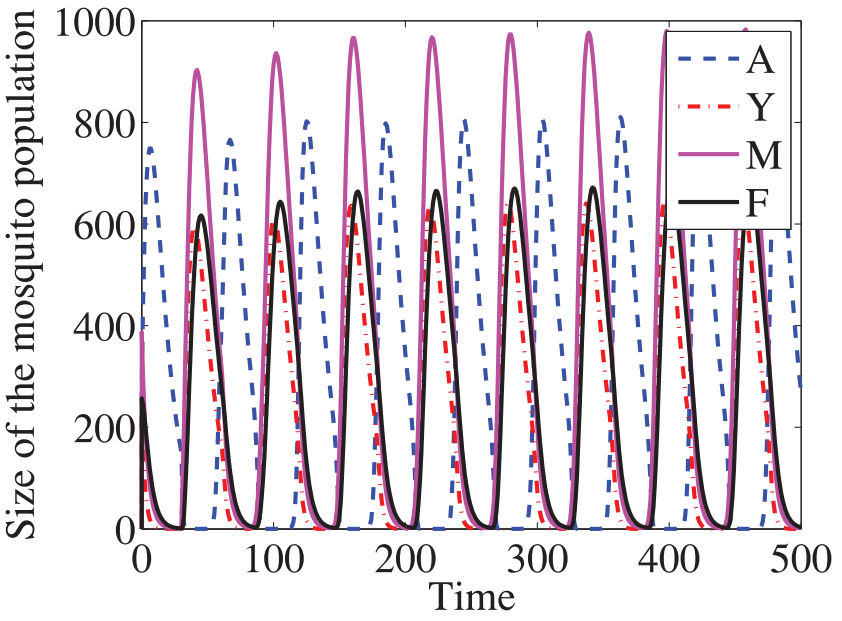

Fig. 8. The impact of the lower environmental temperature (16.1759 °C) and "mild" control regime ($\psi \equiv 30$, $i \equiv 0.2$ and $\alpha \equiv 0.2$) on the stability of the equilibrium $\boldsymbol{X}^* = (280.2290, 236.6077, 387.4125, 257.7628)$. Here, $k = f = 0.9$, $\beta = 0.2643$, $\kappa = 0.6$, the other parameters being given in Table 2. Also, $h = 1$, the solutions being computed by using the NFSD scheme (30). It is observed that $\boldsymbol{X}^*$ repels the solution with the initial conditions $A(t) = 280$, $t \in [-\tau, 0]$, $Y(0) = 236$, $M(0) = 387$ and $F(0) = 257.$.

4. The nonstandard finite difference (NSFD) scheme for the temporal model

In this section, we construct the discrete version of the model (7)–(11) based on the nonstandard finite difference scheme devised by Mickens [48], which was further elaborated by Anguelov and Lubuma [3]. This approach is shown to be more appropriate than the classical Euler or Runge–Kutta approximation schemes because, as far as the existence and positivity of the equilibria are concerned, it is dynamically consistent with the original continuous-time model in (7)–(11), regardless of the step size taken in the numerical simulations (see for example Figs. 13 and 14), as opposed to other numerical schemes. Most importantly, the dynamical consistency guarantees the positivity of solutions (see again Figs. 8–10), contrary to other numerical schemes that may produce negative or spurious solutions. This approximation method is called the NSFD scheme, as explained in [4,26,47], for the following reasons.

- The standard denominator value $\Delta t = h$ of the discrete derivatives is replaced by the more general function $\phi(h)$, which satisfies the requirement $\phi(h) = h + O(h^2)$.
- Nonlinear as well as linear terms are approximated in a nonlocal way by using more than one mesh point.

Because of these advantages, we shall use the NFSD scheme to devise our optimal control strategies.

4.1. The discretized model

Hence, the discretized version of the model (7)–(11) can be given in the following form

$$
\begin{aligned}
\frac{A_{n+1}-A_n}{\phi_1(h,\mu_A,c_M)} &= kf\varphi\left(1-\frac{A_{n+1}}{(1-\frac{\alpha}{\omega})K}\right)F_n-(\mu_A+c_A)A_{n+1}-\eta_A\tilde{A}_n\frac{A_{n+1}}{A_n},\\
\frac{Y_{n+1}-Y_n}{\phi_2(h,\mu_Y,c_M,\beta)} &= \gamma\eta_A\tilde{A}_n-\beta Y_{n+1}-(\mu_Y+c_M)Y_{n+1},\\
\frac{M_{n+1}-M_n}{\phi_3(h,\mu_M,c_M)} &= (1-\gamma)\eta_A\tilde{A}_n-(\mu_M+c_M)M_{n+1},\\
\frac{F_{n+1}-F_n}{\phi_4(h,\mu_F,c_M)} &= \frac{\beta M_{n+1}Y_n}{M_{n+1}+\frac{\kappa\psi}{\mu_S+c_M}}-(\mu_F+c_M)F_{n+1},\\
\frac{U_{n+1}-U_n}{\phi_5(h,\mu_U,c_M)} &= \frac{\beta\frac{\kappa\psi}{\mu_S+c_M}Y_n}{M_{n+1}+\frac{\kappa\psi}{\mu_S+c_M}}-(\mu_U+c_M)U_{n+1}.
\end{aligned}
\tag{30}
$$

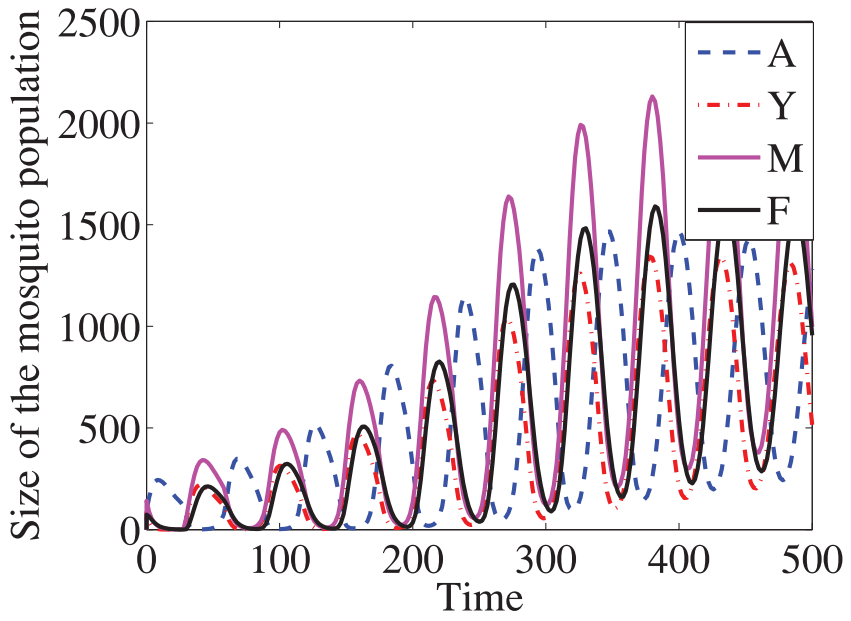

Fig. 9. The impact of the lower environmental temperature (16.5 °C) and "mild" control regime ($\psi \equiv 30$, $i \equiv 0.2$ and $\alpha \equiv 0.2$) on the stability of the equilibrium $\boldsymbol{X}^* = (280.2290, 236.6077, 387.4125, 257.7628)$. Here, $k = f = 0.9$, $\beta = 0.2643$, $\kappa = 0.6$, the other parameters being given in Table 2. Also, $h = 2$, the solutions being computed by using the NFSD scheme (30). It is observed that $\boldsymbol{X}_1^*$ repels the solution with the initial conditions $A(t) = 93$, $t \in [-\tau, 0]$, $Y(0) = 87$, $M(0) = 142$ and $F(0) = 74.$.

In the above,

$$\phi_1(h, \mu_A, c_M) = \frac{e^{(\mu_A + c_M)h} - 1}{(\mu_A + c_M)},$$
$$\phi_2(h, \mu_Y, c_M, \beta) = \frac{e^{(\mu_Y + c_M + \beta)h} - 1}{(\mu_Y + c_M + \beta)},$$
$$\phi_3(h, \mu_M, c_M) = \frac{e^{(\mu_M + c_M)h} - 1}{(\mu_M + c_M)},$$
$$\phi_4(h, \mu_F, c_M) = \frac{e^{(\mu_F + c_M)h} - 1}{(\mu_F + c_M)},$$
$$\phi_5(h, \mu_U, c_M) = \frac{e^{(\mu_U + c_M)h} - 1}{(\mu_U + c_M)},$$
$$\tilde{A}_n \approx A(t_n - \tau) = (1 - u)A_{n-l-1} + uA_{n-l}.$$

Here and after, $A_n = A(t_n)$ and $Y_n = Y(t_n)$, $M_n = M(t_n)$, $F_n = F(t_n)$, $U_n = U(t_n)$ are the number of mosquitos in the aquatic phase and adult stage, respectively, at time $t_n = n\Delta t$ as in the continuous model. Using the approach for discretization of delay term in [25], we approximate the delay term $A(t_n - \tau)$ by $\tilde{A}_n$. For a given step size h and delay τ, we define $l = [\frac{\tau}{h}]$, the integer part of $\frac{\tau}{h}$ and $u = \frac{(l+1)h - \tau}{h}$. All other parameters have the same meaning and values as in Table 2.

4.2. Positivity of solutions

In this section, we show that the NSFD scheme replicates the positivity of solutions, as claimed in Section 2.3. We state the following result:

Theorem 4.1. *Given the positive initial conditions Y_0, M_0, F_0, U_0 and A_{-l-1}, $A_{-l}, \ldots, A_0$, the solutions A_n, Y_n, M_n, F_n, U_n of the discretized model (30) are positive at all times t_n, for $n = 1, 2, \ldots$.*

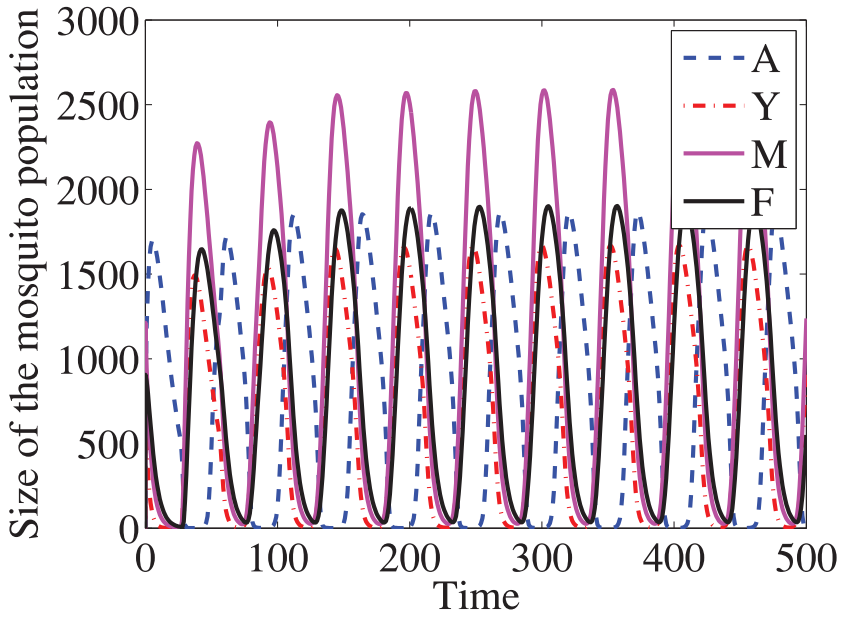

Fig. 10. The impact of the lower environmental temperature (16.5 °C) and "mild" control regime ($\psi \equiv 30$, $i \equiv 0.2$ and $\alpha \equiv 0.2$) on the stability of the equilibrium $\boldsymbol{X}^* = (280.2290, 236.6077, 387.4125, 257.7628)$. Here, $k = f = 0.9$, $\beta = 0.2643$, $\kappa = 0.6$, the other parameters being given in Table 2. Also, $h = 1$, the solutions being computed by using the NFSD scheme (30). It is observed that $\boldsymbol{X}_1^*$ repels the solution with the initial conditions $A(t) = 791$, $t \in [-\tau, 0]$, $Y(0) = 740$, $M(0) = 1212$ and $F(0) = 905$.

Table 2
State variables and parameters of the model (values of the parameters and initial state variables used in the numerical simulations).

Symbol	Quantity	Default value	Dimensions	Sources
A	Aquatic phase	Variable	Aquatic forms	
Y	Unmating female mosquitoes	Variable	Females	
M	Wild male mosquitoes	Variable	Males	
F	Mating fertilized female mosquitoes	Variable	Females	
U	Mating unfertilized female mosquitoes	Variable	Females	
S	Sterile male mosquitoes	Variable	Males	
k	Fraction of eggs hatching to larvae	(0,1)		[65]
f	Fraction of female mosquitoes hatched from all eggs	(0,1)		[65]
φ	Oviposition rate	Fig. 5	Aquatic forms female^{-1} day^{-1}	[65]
α	Proportion of mechanical control (control variable)	[0, 1]		
K	Carrying capacity	Fig. 4	Aquatic forms	
μ_A	Mortality rate of aquatic forms	Fig. 6	day^{-1}	[65]
μ_Y	Mortality rate of unmating females	Fig. 6	day^{-1}	[65]
β	Total mating rate	$\frac{1}{3.33} - \mu_Y$	day^{-1}	[13]
μ_M	Mortality rate of wild males	$\frac{1}{7}$	day^{-1}	[13]
μ_F	Mortality rate of mating fertilized females	0.1	day^{-1}	[13]
μ_U	Mortality rate of mating unfertilized females	–	day^{-1}	
μ_S	Mortality rate of sterile males	$\frac{1}{7}$	day^{-1}	[13]
η_A	Survival rate from larvae to adult	Fig. 2	day^{-1}	
$\frac{1-\gamma}{\gamma}$	Ratio of male to female mosquitoes	1		
τ	Mean instar duration	Fig. 5	Days	[43]
κ	Actual effective mating competitiveness of the sterile males	(0,1)		
$\psi(t)$	Release rate of sterile males (control variable)	> 0	Males day^{-1}	
c_A	Larvicide-related death rate	(0, 1)	Day^{-1}	
c_M	Adulticide-related death rate	(0, 1)	Day^{-1}	
T	Ambient temperature	[15, 35]	°C	[43]
ω	Rescaling constant	2		

- "–" represents that, in the following sections, the value of this parameter will not be surveyed in detail;
- c_A and c_M both depend on the pesticide dosage function $i(t)$, which is a control variable;
- At 10 °C and 40 °C, all immature mosquitoes would die in the first instar [43].

Proof. Assuming we have positive initial data for the model (30), by solving the model equations at step $n+1$, we obtain that

$$\begin{aligned}
A_{n+1} &= \frac{A_n + (kf\varphi F_n)\phi_1}{1 + \frac{(kf\varphi F_n)\phi_1}{(1-\frac{\alpha}{\omega})K} + (\mu_A + c_A)\phi_1 + \frac{\phi_1\eta_A((1-u)A_{n-l-1}+uA_{n-l})}{A_n}} \doteq g(A_n, F_n, A_{n-l-1}, A_{n-l}),\\
Y_{n+1} &= \frac{Y_n + \phi_2\gamma\eta_A((1-u)A_{n-l-1} + uA_{n-l})}{1 + \phi_2(\beta + \mu_Y + c_M)} \doteq j(Y_n, A_{n-l-1}, A_{n-l}),\\
M_{n+1} &= \frac{M_n + \phi_3(1-\gamma)\eta_A((1-u)A_{n-l-1} + uA_{n-l})}{1 + \phi_3(\mu_M + c_M)} \doteq p(M_n, A_{n-l-1}, A_{n-l}),\\
F_{n+1} &= \frac{F_n + \frac{\phi_4\beta M_{n+1}Y_n}{M_{n+1} + \frac{\kappa\psi}{\mu_S + c_M}}}{1 + \phi_4(\mu_F + c_M)} \doteq q(F_n, Y_n, M_{n+1})\\
U_{n+1} &= \frac{U_n + \frac{\frac{\phi_5\beta\kappa\psi Y_n}{\mu_S + c_M}}{M_{n+1} + \frac{\kappa\psi}{\mu_S + c_M}}}{1 + \phi_5(\mu_U + c_M)} \doteq w(U_n, Y_n, M_{n+1}).
\end{aligned} \tag{31}$$

The desired positivity property follows now from an easy induction argument. Therefore, the solution of the model (30) is always positive whenever we start with positive initial data. □

4.3. The fixed points of the NFSD model

The fixed points for the NSFD model (which are the corresponding equilibria of the continuous model) can be obtained by solving the following system of algebraic equations:

$$\begin{aligned}
A^* &= g(A^*, F^*, A^*, A^*)\\
Y^* &= j(Y^*, A^*, A^*)\\
M^* &= p(M^*, A^*, A^*)\\
F^* &= q(F^*, Y^*, M^*)\\
U^* &= w(U^*, Y^*, M^*).
\end{aligned} \tag{32}$$

It is easy to see that the system (31) has the trivial solution $\mathbf{0} = (0, 0, 0, 0, 0)$. As for the positive (component-wise) solution, the values are determined as shown below:

From the third equation in (31), we have

$$M^* = \frac{(1-\gamma)\eta_A A^*}{(\mu_M + c_M)}. \tag{33}$$

Also, solving the second equation in (31) for Y^*, it implies

$$Y^* = \frac{\gamma\eta_A A^*}{(\beta + \mu_Y + c_M)}. \tag{34}$$

And from the fourth equation of (31), we have

$$F^* = \frac{\beta M^* Y^*}{(\mu_F + c_M)(M^* + \frac{\kappa\psi}{\mu_S + c_M})}. \tag{35}$$

From the last equation of (31), solving for U^*:

$$U^* = \frac{\frac{\beta\kappa\psi}{\mu_S + c_M}Y^*}{(\mu_U + c_M)(M^* + \frac{\kappa\psi}{\mu_S + c_M})}. \tag{36}$$

Now, if we substitute Eqs. (33) and (34) into (35), after simplification, F^* is given again by

$$F^* = \frac{\beta\gamma\eta_A A^{*2}}{(\beta + \mu_Y + c_M)[(\mu_F + c_M)A^* + Q]}, \tag{37}$$

and substituting this value of F^* in the first equation of (31) and simplifying, it can be seen that A^* is the positive solution of the quadratic equation

$$A^{*2}\mathcal{R} - A^*(\mathcal{R} - 1)P + PQ = 0, \tag{38}$$

where P, Q and $\mathcal{R}$ have the same values as in Eqs. (14) and (12) respectively.

Therefore, the corresponding fixed point for the NSFD scheme (31) is given by $\boldsymbol{X}^* = (A^*, Y^*, M^*, F^*, U^*)$, where

$$
\begin{aligned}
Y^* &= \frac{\gamma\eta_A}{\beta+\mu_Y+c_M}A^*,\\
M^* &= \frac{(1-\gamma)\eta_A}{\mu_M+c_M}A^*,\\
F^* &= \frac{\beta M^*}{(\mu_F+c_M)M^*+\frac{\kappa\psi}{\mu_S+c_M}}Y^*,\\
U^* &= \frac{\beta\frac{\kappa\psi}{\mu_S+c_M}}{(\mu_U+c_M)(M^*+\frac{\kappa\psi}{\mu_S+c_M})}Y^*,
\end{aligned}
\tag{39}
$$

with A^* being a root of (38) whenever $\mathcal{R} > 1$. Hence we claim that the fixed points of NSFD scheme (31) coincide with the equilibria of (13).

4.4. Transforming the NSFD model into a delay-free model

As pointed out in Dadebo and Luus [16], certain difficulties arise when applying iterative dynamical programming (IDP) to solve time-delayed optimal control problems. We therefore use the idea proposed by Chen *et al.* [12], in which a time-delayed system is transformed into an augmented, delay-free system by using linearly truncated Taylor series expansions. The time-delayed terms are then replaced by the augmented auxiliary states.

We assume that the time delay τ is divided into L sections and hence L auxiliary states are used to represent the state values at different intervals as shown below

$$
A_l(t) = A\left(t-\frac{l}{L}\tau\right), \quad l = 0, 1, 2, \cdots, L. \tag{40}
$$

For the sake of simplicity, setting $L = 2$, we have

$$
\begin{aligned}
A_{m2}(t) &= A(t-\tau),\\
A_{m1}(t) &= A\left(t-\frac{\tau}{2}\right),\\
A_{m0}(t) &= A(t).
\end{aligned}
\tag{41}
$$

Equivalently,

$$
\begin{aligned}
A_{m1}(t+\frac{\tau}{4}) &= A\left(t-\frac{\tau}{4}\right)\\
A_{m2}(t+\frac{\tau}{2}) &= A\left(t-\frac{\tau}{2}\right)\\
A_{m2}(t) &= A_{m1}\left(t-\frac{\tau}{2}\right).
\end{aligned}
\tag{42}
$$

From the above, using first order Taylor expansions, we obtain

$$
\begin{aligned}
A_{m1}(t)+\frac{\tau}{4}\dot{A}_{m1}(t) &= A(t)-\frac{\tau}{4}\dot{A}(t),\\
A_{m2}(t)+\frac{\tau}{4}\dot{A}_{m2}(t) &= A_{m1}(t)-\frac{\tau}{4}\dot{A}_{m1}(t),
\end{aligned}
\tag{43}
$$

where $\dot{A}_{m1}$, $\dot{A}_{m2}$ represent derivatives with respect to time of A_{m1}, A_{m2} respectively.

Solving for $\dot{A}_{m1}(t)$ and $\dot{A}_{m2}(t)$, it is seen that

$$
\begin{aligned}
\dot{A}_{m2}(t) &= \frac{4}{\tau}[2A_{m1}(t)-A_{m2}(t)-A(t)]+\dot{A}(t),\\
\dot{A}_{m1}(t) &= \frac{4}{\tau}[A(t)-A_{m1}(t)]-\dot{A}(t).
\end{aligned}
\tag{44}
$$

Using the properties of the auxiliary states given in (44) and (41), we now add the auxiliary states and replace the delay terms in (30).

The discretized NSFD version of the delay–free model can then be given in the following form

$$\begin{aligned}
\frac{A_{m1,n+1}-A_{m1,n}}{\phi_1(h,\tau)} &= \frac{4}{\tau}[A_n - A_{m1,n+1}] - \left(\frac{A_{n+1}A_{m1,n+1}}{A_{m1,n}\phi_2(h,\mu_A,c_A)} - \frac{A_n}{\phi_2(h,\mu_A,c_A)}\right),\\
\frac{A_{m2,n+1}-A_{m2,n}}{\phi_1(h,\tau)} &= \frac{4}{\tau}\left[2A_{m1,n} - A_{m2,n} - A_n\frac{A_{m2,n+1}}{A_{m2,n}}\right] + \frac{A_{n+1}-A_n}{\phi_2(h,\mu_A,c_A)},\\
\frac{A_{n+1}-A_n}{\phi_2(h,\mu_A,c_A)} &= kf\varphi\left(1-\frac{A_{n+1}}{(1-\frac{\alpha}{\omega})K}\right)F_n - (\mu_A+c_A)A_{n+1} - \eta_A A_{m2,n}\frac{A_{n+1}}{A_n},\\
\frac{Y_{n+1}-Y_n}{\phi_3(h,\mu_Y,c_M,\beta)} &= \gamma\eta_A A_{m2,n} - \beta Y_{n+1} - (\mu_Y+c_M)Y_{n+1},\\
\frac{M_{n+1}-M_n}{\phi_4(h,\mu_M,c_M)} &= (1-\gamma)\eta_A A_{m2,n} - (\mu_M+c_M)M_{n+1},\\
\frac{F_{n+1}-F_n}{\phi_5(h,\mu_F,c_M)} &= \frac{\beta M_{n+1}Y_n}{M_{n+1}+\frac{\kappa\psi}{\mu_S+c_M}} - (\mu_F+c_M)F_{n+1},\\
\frac{U_{n+1}-U_n}{\phi_6(h,\mu_U,c_M)} &= \frac{\beta\frac{\kappa\psi}{\mu_S+c_M}Y_n}{M_{n+1}+\frac{\kappa\psi}{\mu_S+c_M}} - (\mu_U+c_M)U_{n+1}.
\end{aligned} \tag{45}$$

In the above,

$$\begin{aligned}
\phi_1(h,\tau) &= \frac{e^{\frac{4h}{\tau}}-1}{\frac{4}{\tau}},\\
\phi_2(h,\mu_A,c_M) &= \frac{e^{(\mu_A+c_M)h}-1}{(\mu_A+c_M)},\\
\phi_3(h,\mu_Y,c_M,\beta) &= \frac{e^{(\mu_Y+c_M+\beta)h}-1}{(\mu_Y+c_M+\beta)},\\
\phi_4(h,\mu_M,c_M) &= \frac{e^{(\mu_M+c_M)h}-1}{(\mu_M+c_M)},\\
\phi_5(h,\mu_F,c_M) &= \frac{e^{(\mu_F+c_M)h}-1}{(\mu_F+c_M)},\\
\phi_6(h,\mu_U,c_M) &= \frac{e^{(\mu_U+c_M)h}-1}{(\mu_U+c_M)}.
\end{aligned}$$

By solving the equations in the transformed delay-free model (45) for $(A, A_{m1}, A_{m2}, Y, M, F, U)$ at the node $n+1$, it can be seen that the discretizations in (45), preserve the positivity of the solutions, as it happened with the NSFD model (30) and the continuous model. Similarly, considering the system (45) without the two auxiliary states A_{m1} and A_{m2}, the discretizations of other variables are the same as in the NSFD model (30). Therefore, the proposed model (45) again has the same dynamical consistency in terms of positivity and existence of equilibria as the continuous model system (1)–(6) irrespective of the step size used. These two assertions are verified numerically in Figs. 8–10 and 13 and 14.

5. Optimal *Aedes aegypti* mosquito control regime

So far, we have investigated the dynamics of continuous and discrete models of *Aedes aegypti* mosquito control subject to three control mechanisms: pesticide release, mechanical control and the sterile insect technique (SIT). The optimal control problem can be posed as the following question: What is the best combined control regime of pesticide release, mechanical control and SIT for the discrete model described above so that the population size of the aquatic phase is reduced to the minimal level?

Since it has already been shown in Section 4 that the time-delayed system can be transformed into an augmented, delay-free discrete system by using a linearly truncated Taylor series expansion, we now focus on the delay-free optimal control problem with augmented states, which can be solved by means of the discrete minimum principle introduced by Goodwin *et al.* in [28].

Even though optimal control for systems of difference equations seems to be an adequate tool in the biosciences, there are relatively few studies in this area. In our case, the control variable α represents the mechanical control and i represents the pesticide dosage function. Meanwhile, ψ gives information about the human intervention mechanisms, in form of the release rate of sterile mosquitoes. We wish to minimize the cost of insecticides, of using mechanical controls and of releasing mosquitoes, as well as the population size of the aquatic phase. To this end, we define

$$\{X_n\} \doteq \left\{[X_n^1, X_n^2, X_n^3, X_n^4, X_n^5, X_n^6, X_n^7]^{\mathbf{T}}\right\} \doteq \left\{[A_{m1,n}, A_{m2,n}, A_n, Y_n, M_n, F_n, U_n]^{\mathbf{T}}\right\}, \tag{46}$$

in which $B^{\mathbf{T}}$ denotes the transpose of a matrix B, $n = 0, 1, \ldots, N$, and

$$\{V_n\} \doteq \left\{[V_n^1, V_n^2, V_n^3]^{\mathbf{T}}\right\} \doteq \left\{[\alpha_n, i_n, \psi_n]^{\mathbf{T}}\right\}, \tag{47}$$

in which $n = 0, 1, \ldots, N-1$. Here, N is the optimization horizon. Our problem may then be stated as

$$\text{Minimize } \mathcal{V}_N(X_n, V_n) = A_N + \Sigma_{n=0}^{N-1}(A_n + c_\alpha \alpha_n^2 + c_i i_n^2 + c_\psi \psi_n^2) \tag{48}$$

subject to

$$\begin{aligned}
X_{n+1}^1 &= A_{m1,n+1} = \frac{A_{m1,n} + [\frac{4}{\tau} + \frac{1}{\phi_2}]\phi_1 A_n}{(1 + \frac{4\phi_1}{\tau} + \frac{f_A(A_{m2,n}, A_n, F_n, \alpha_n, i_n)\phi_1}{A_{m1,n}\phi_2})} \doteq \mathcal{G}_1(X_n, V_n),\\
X_{n+1}^2 &= A_{m2,n+1} = \frac{A_{m2,n}(1 - \frac{4\phi_1}{\tau}) + \frac{8\phi_1 A_{m1,n}}{\tau} + \frac{(f_A(A_{m2,n}, A_n, F_n, \alpha_n, i_n) - A_n)\phi_1}{\phi_2^n}}{1 + \frac{4}{\tau}\frac{A_n \phi_1}{A_{m2,n}}} \doteq \mathcal{G}_2(X_n, V_n),\\
X_{n+1}^3 &= A_{n+1} = \frac{A_n + (kf\varphi F_n)\phi_2^n}{1 + \frac{(kf\varphi F_n)\phi_2^n}{(1 - \frac{\alpha_n}{\omega})K} + (\mu_A + c_A^n)\phi_2^n + \frac{\phi_2^n \eta_A A_{m2,n}}{A_n}} \doteq \mathcal{G}_3(X_n, V_n),\\
X_{n+1}^4 &= Y_{n+1} = \frac{Y_n + \phi_3^n \gamma \eta_A A_{m2,n}}{1 + \phi_3^n(\beta + \mu_Y + c_M^n)} \doteq \mathcal{G}_4(X_n, V_n),\\
X_{n+1}^5 &= M_{n+1} = \frac{M_n + \phi_4^n(1-\gamma)\eta_A A_{m2,n}}{1 + \phi_4^n(\mu_M + c_M^n)} \doteq \mathcal{G}_5(X_n, V_n),\\
X_{n+1}^6 &= F_{n+1} = \frac{F_n + \frac{\phi_5^n \beta \mathcal{G}_5(X_n, V_n) Y_n}{\mathcal{G}_5(X_n, V_n) + \frac{\kappa \psi_n}{\mu_S + c_M^n}}}{1 + \phi_5^n(\mu_F + c_M^n)} \doteq \mathcal{G}_6(X_n, V_n),\\
X_{n+1}^7 &= U_{n+1} = \frac{U_n + \frac{\phi_6^n \frac{\beta \kappa \psi_n}{\mu_S + c_M^n} Y_n}{\mathcal{G}_5(X_n, V_n) + \frac{\kappa \psi_n}{\mu_S + c_M^n}}}{1 + \phi_6^n(\mu_U + c_M^n)} \doteq \mathcal{G}_7(X_n, V_n),\\
X_0 &= \overline{X},
\end{aligned} \tag{49}$$

in which $f_A(A_{m2,n}, A_n, F_n, \alpha_n, i_n) = \mathcal{G}_3(X_n, V_n)$, c_α, c_i and c_ψ are the costs of using mechanical controls, of spraying insecticides and of releasing sterile mosquitoes, respectively. Also, $\overline{X}$ is the initial state and

$$\begin{aligned}
c_A^n &= 1 - \exp(-\gamma_A i_n + \delta_A),\\
c_M^n &= 1 - \exp(-\gamma_M i_n + \delta_M),\\
\phi_2^n &= \frac{e^{(\mu_A + c_M^n)h} - 1}{(\mu_A + c_M^n)},\\
\phi_3^n &= \frac{e^{(\mu_Y + c_M^n + \beta)h} - 1}{(\mu_Y + c_M^n + \beta)},\\
\phi_4^n &= \frac{e^{(\mu_M + c_M^n)h} - 1}{(\mu_M + c_M^n)},\\
\phi_5^n &= \frac{e^{(\mu_F + c_M^n)h} - 1}{(\mu_F + c_M^n)},\\
\phi_6^n &= \frac{e^{(\mu_U + c_M^n)h} - 1}{(\mu_U + c_M^n)}.
\end{aligned}$$

In order to apply the Karush–Kuhn–Tucker (KKT) optimality conditions, we need to verify the constraint qualification that the gradients of the equality constraints be linearly independent when evaluated at the minimizers. Subsequently, we define a new variable

$$X \doteq \left[X_0^{\mathbf{T}}, X_1^{\mathbf{T}}, \ldots, X_N^{\mathbf{T}}, V_0^{\mathbf{T}}, V_1^{\mathbf{T}}, \ldots, V_{N-1}^{\mathbf{T}}\right]^{\mathbf{T}} \in \mathbf{R}^{10N+7}, \tag{50}$$

which comprises all the variables with respect to which the optimization is performed. Now let

$$\mathcal{G}(X_n, V_n) = \left[\mathcal{G}_1(X_n, V_n), \mathcal{G}_2(X_n, V_n), \ldots, \mathcal{G}_7(X_n, V_n)\right]^{\mathbf{T}}.$$

We can then write the state equations (49) as $7(N+1)$ equality constraints on X as follows

$$h(X)=\begin{bmatrix}h_0\\h_1\\\vdots\\h_N\end{bmatrix}=\begin{bmatrix}\overline{X}-X_0\\\mathcal{G}(X_0,V_0)-X_1\\\vdots\\\mathcal{G}(X_{N-1},V_{N-1})-X_N\end{bmatrix}=0. \tag{51}$$

Also, we define

$$\frac{\partial\mathcal{G}}{\partial X_n}=\begin{bmatrix}\frac{\partial\mathcal{G}_1}{\partial X_n^1}&\cdots&\frac{\partial\mathcal{G}_1}{\partial X_n^7}\\\vdots&\vdots&\vdots\\\frac{\partial\mathcal{G}_7}{\partial X_n^1}&\cdots&\frac{\partial\mathcal{G}_7}{\partial X_n^7}\end{bmatrix}\text{ and }\frac{\partial\mathcal{G}}{\partial \mathrm{V_n}}=\begin{bmatrix}\frac{\partial\mathcal{G}_1}{\partial V_n^1}&\frac{\partial\mathcal{G}_1}{\partial V_n^2}&\frac{\partial\mathcal{G}_1}{\partial V_n^3}\\\vdots&\vdots&\vdots\\\frac{\partial\mathcal{G}_7}{\partial V_n^1}&\frac{\partial\mathcal{G}_7}{\partial V_n^2}&\frac{\partial\mathcal{G}_7}{\partial V_n^3}\end{bmatrix} \tag{52}$$

for $n=0,1,\ldots,N-1$. We then compute the $(7N+7)\times(10N+7)$ Jacobian matrix of the vector-valued function $h(X)$ as being

$$\frac{\partial h}{\partial X}=\begin{bmatrix}-\mathrm{I}_7&\mathbf{0}&\mathbf{0}&\cdots&\mathbf{0}&\mathbf{0}&\mathbf{0}&\mathbf{0}&\cdots&\mathbf{0}\\\frac{\partial\mathcal{G}}{\partial X_0}&-\mathrm{I}_7&\mathbf{0}&\cdots&\mathbf{0}&\mathbf{0}&\frac{\partial\mathcal{G}}{\partial V_0}&\mathbf{0}&\cdots&\mathbf{0}\\\mathbf{0}&\frac{\partial\mathcal{G}}{\partial X_1}&-\mathrm{I}_7&\cdots&\mathbf{0}&\mathbf{0}&\mathbf{0}&\frac{\partial\mathcal{G}}{\partial V_1}&\cdots&\mathbf{0}\\\vdots&\vdots&\vdots&\ddots&\vdots&\vdots&\vdots&\vdots&\ddots&\vdots\\\mathbf{0}&\mathbf{0}&\mathbf{0}&\cdots&\frac{\partial\mathcal{G}}{\partial X_{N-1}}&-\mathrm{I}_7&\mathbf{0}&\mathbf{0}&\cdots&\frac{\partial\mathcal{G}}{\partial V_{N-1}}\end{bmatrix}, \tag{53}$$

in which $\mathbf{0}$ denotes zero matrices of appropriate dimensions, and I_7 denotes the 7×7 identity matrix. Since the matrix $\frac{\partial h}{\partial X}$ in (54) has full row rank for all $X\in\mathbf{R}^{10N+7}$, the gradients of the equality constraints (52) are linearly independent, which implies that the constraint qualification required by the KKT optimality conditions of Theorem 2.5.5 in [28] holds for all $X\in\mathbf{R}^{10N+7}$.

Next, we introduce the Lagrange multipliers $\lambda_{-1}\in\mathbf{R}^7$ for the initial state equation,

$$\{\lambda_n\}=\{\lambda_0,\lambda_1,\ldots,\lambda_{N-1}\},\quad \{\lambda_n\}\in\mathbf{R}^N$$

(usually referred to as adjoint variables) for the state equations, $\lambda=[\lambda_{-1}^{\mathbf{T}},\lambda_0^{\mathbf{T}},\ldots,\lambda_{N-1}^{\mathbf{T}}]^{\mathbf{T}}$, and the Hamiltonian $\mathcal{H}:\mathbf{R}^{7N+7}\times\mathbf{R}^{3N}\times\mathbf{R}^7\to\mathbf{R}$ defined as

$$\mathcal{H}(X_n,V_n,\lambda_n)=X_N^3+\Sigma_{n=0}^{N-1}\left(X_n^3+c_\alpha(V_n^1)^2+c_i(V_n^2)^2+c_\psi(V_n^3)^2\right)+\lambda_{-1}^{\mathbf{T}}h_0+\Sigma_{k=0}^{N-1}\lambda_k h_{k+1}. \tag{54}$$

According to the KKT conditions, we obtain the following necessary condition for the existence of optimal mosquito population control.

Theorem 5.1. *A necessary condition for*

$$X^*\doteq\left[(X_0^*)^{\mathbf{T}},(X_1^*)^{\mathbf{T}},\ldots,(X_N^*)^{\mathbf{T}},(V_0^*)^{\mathbf{T}},(V_1^*)^{\mathbf{T}},\ldots,(V_{N-1}^*)^{\mathbf{T}}\right]^{\mathbf{T}} \tag{55}$$

to be the minimizing vector corresponding to the state variable sequences $\{X_0^*,X_1^*,\ldots,X_N^*\}$ *and the control variable sequence* $\{V_0^*,V_1^*,\ldots,V_{N-1}^*\}$ *that minimize the control problem (48)–(49) is that there exists a sequence of Lagrange multipliers*

$$\left\{\lambda_{-1}^*,\lambda_0^*,\cdots,\lambda_{N-1}^*\right\}$$

such that

(i) X^* *satisfies the state equations (49);*
(ii) $(\lambda_{n-1}^*)^{\mathbf{T}}=\frac{\partial\mathcal{H}}{\partial X_n}(X^*,\lambda_n^*)$ *for* $n=0,1,\ldots,N-1$;
(iii) $(\lambda_{N-1}^*)^{\mathbf{T}}=\frac{\partial X_N^{3^*}}{\partial X_N}$;
(iv) $\frac{\partial\mathcal{H}}{\partial V_n}(X^*,\lambda_n^*)=0$ *for* $n=0,1,\ldots,N-1$.

6. Numerical simulations

In this section, we study from a numerical viewpoint the stability of the equilibria, as well as the outcome of the optimal combined controls under different environmental temperatures. It is important to select appropriate parameter values, since they make a difference in various aspects regarding the dynamics of the delay differential system (the number of fixed points and stability of each, among other things).

First of all, we wish to study numerically the behavioral patterns that can arise within this model when using a range of "reasonable" parameter values together with the values given in Table 2. To illustrate the stability of the equilibrium point of the system (7)–(10), the numerical particulars of different control regimes under different environmental temperatures are given as follows.

Scheme 1 Considering the "mild" control regime ($i=0.2$, $\alpha=0.2$ and $\psi=30$) under varying temperature (T varies from 15 °C to 35 °C, which indicates that the delay τ changes from 39.7121 to 7.1093 as shown in Fig. 5), we obtain that the

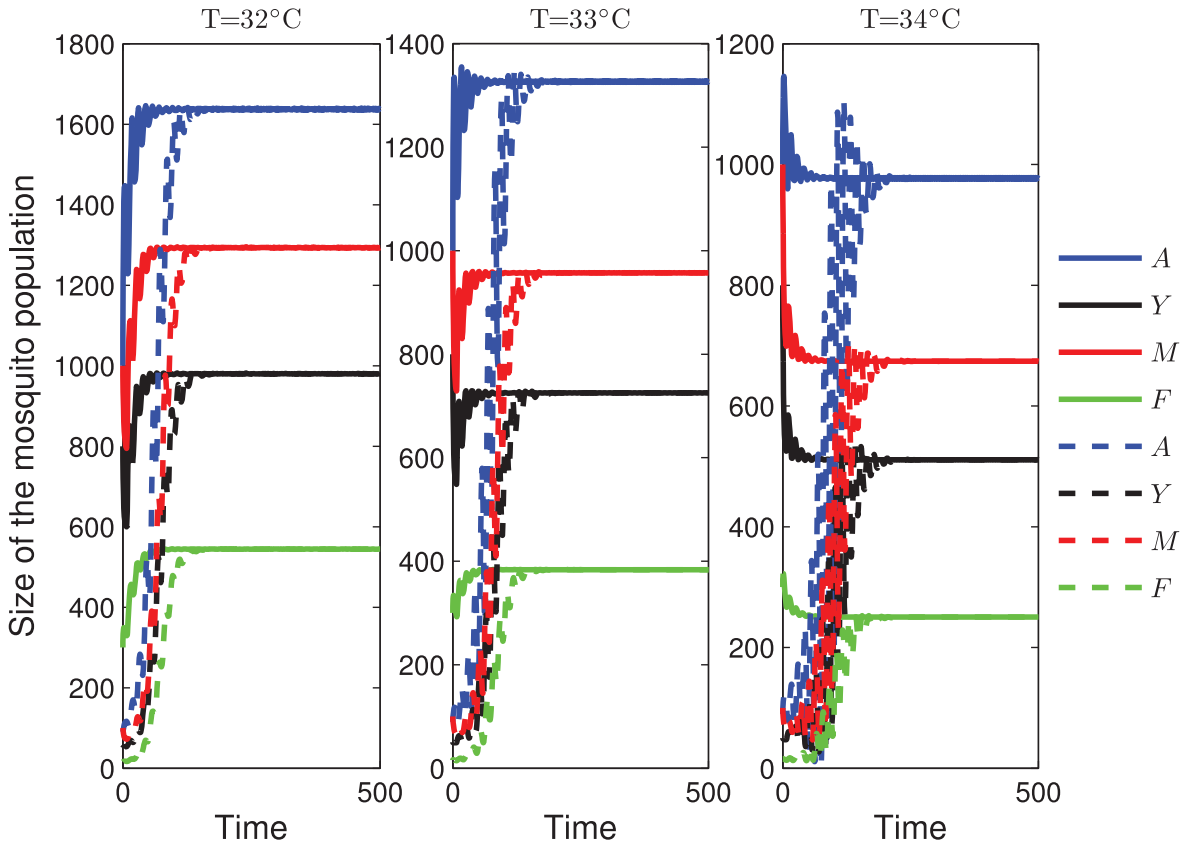

Fig. 11. The impact of the varying environmental temperature and "medium" control regime ($\psi \equiv 50$, $i \equiv 0.6$ and $\alpha \equiv 0.8$) on the stability of the equilibria. Here, $k = f = 0.9$, $\kappa = 0.6$, the other parameters being given in Table 2. The equilibrium $\boldsymbol{X}_2^*$ is locally stable, while $\mathbf{0}$ and $\boldsymbol{X}_1^*$ are unstable. Here, when $T = 32\,^\circ$C and $\eta_A = 0.7778$, $\mu_A = 0.0698$, $c_A = 0.3560$, $\tau = 7.5902$, $\tau^* = 3.3026$, $\beta = 0.2615$ one obtains the positive equilibria $\boldsymbol{X}_1^* = (73.1561, 43.7858, 57.7876, 12.3989)$ and $\boldsymbol{X}_2^* = (1637.2, 979.8940, 1293.2, 544.4055)$. It is observed that $\boldsymbol{X}_2^*$ is locally stable, attracting the solutions with the initial conditions $A(t) = 1000$, $t \in [-\tau, 0]$, $Y(0) = 800$, $M(0) = 1000$ and $F(0) = 300$ (solid curves) and, respectively, the initial conditions $A(0) = 90$, $t \in [-\tau, 0]$, $Y(0) = 50$, $M(0) = 100$ and $F(0) = 16$ (dashed curves). When $T = 33\,^\circ$C and $\eta_A = 0.7104$, $\mu_A = 0.0732$, $c_A = 0.3560$, $\tau = 7.2452$, $\tau^* = 3.9205$, $\beta = 0.2530$, one obtains the positive equilibria $\boldsymbol{X}_1^* = (84.0891, 45.9661, 60.6651, 12.9054)$ and $\boldsymbol{X}_2^* = (1326.8, 725.2508, 957.1717, 383.7121)$. It is observed that $\boldsymbol{X}_2^*$ is locally stable, attracting the solutions with the initial conditions $A(t) = 1000$, $t \in [-\tau, 0]$, $Y(0) = 800$, $M(0) = 1000$ and $F(0) = 300$ (solid curves) and, respectively, the initial conditions $A(0) = 90$, $t \in [-\tau, 0]$, $Y(0) = 50$, $M(0) = 100$ and $F(0) = 16$ (dashed curves). When $T = 33\,^\circ$C and $\eta_A = 0.6794$, $\mu_A = 0.0798$, $c_A = 0.3560$, $\tau = 7.1093$, $\tau^* = 4.3503$, $\beta = 0.2404$, one obtains the positive equilibria $\boldsymbol{X}_1^* = (95.0257, 49.6748, 65.5598, 13.7669)$ and $\boldsymbol{X}_2^* = (977.0405, 510.7485, 674.0758, 250.4672)$. It is observed that $\boldsymbol{X}_2^*$ is locally stable, attracting the solutions with the initial conditions $A(t) = 1000$, $t \in [-\tau, 0]$, $Y(0) = 800$, $M(0) = 1000$ and $F(0) = 300$ (solid curves) and, respectively, the initial conditions $A(0) = 90$, $t \in [-\tau, 0]$, $Y(0) = 50$, $M(0) = 100$ and $F(0) = 16$ (dashed curves). .

value of $\mathcal{R}$ linearly increases from 0.2854 to 3.95 and then decreases up to 3.786. If $T = 16.1759\,^\circ$C, such that $\mathcal{R} = \mathcal{R}_2^* = 1.3727$, $\eta_A = 0.6830 > \mu_A(0.0257) + c_A(0.0769)$ and $\tau = 29.9901 > \tau^* = 2.5496$, then the equilibria $\mathbf{0}$ and $\boldsymbol{X}^*$ are unstable (see Fig. 8). If $T = 16.5\,^\circ$C, then $\tau = 27.7870$. Figs. 9 and 10 show that the equilibria $\boldsymbol{X}_1^*$ and $\boldsymbol{X}_2^*$ are also unstable.

Scheme 2 Consider the "medium" control regimes ($i = 0.6$, $\alpha = 0.8$ and $\psi = 50$) under varying temperature. If $T = 32\,^\circ$C, then $\tau = 7.5902 > \tau^* = 3.3026$, $\eta_A = 0.7778 > \mu_A(0.0698) + c_A(0.3560)$ and $\mathcal{R} = 2.1015$; If $T = 33\,^\circ$C, then $\tau = 7.2452 > \tau^* = 3.9205$, $\eta_A = 0.7104 > \mu_A(0.0732) + c_A(0.3560)$ and $\mathcal{R} = 2.0681$; If $T = 34\,^\circ$C, then $\tau = 7.1093 > \tau^* = 4.3503$, $\eta_A = 0.6794 > \mu_A(0.0798) + c_A(0.3560)$ and $\mathcal{R} = 2.0198$. Fig. 11 shows that only $\boldsymbol{X}_2^*$ is locally asymptotically stable, while $\mathbf{0}$ and $\boldsymbol{X}_1^*$ are unstable.

Since our NSFD discrete model is shown to be dynamically consistent with the continuous delay model as far as the positivity of solutions, existence and local stability properties of equilibria are concerned, we hereby illustrate the consistency of the dynamical behavior under varying environmental temperatures in Fig. 12. Secondly, using combinations of the three controls α_n, i_n and ψ_n under different temperatures, we investigate and compare numerical results from simulations with the following two scenarios.

(a) Considering different environmental temperatures $T = 24\,^\circ$C, $28\,^\circ$C and $32\,^\circ$C, respectively, and using the mechanical control α_n, the pesticide control i_n and the human intervention control mechanisms ψ_n;
(b) Considering different environmental temperatures $T = 24\,^\circ$C, $28\,^\circ$C and $32\,^\circ$C, respectively, and using minimal levels of combined controls ($\alpha_n \equiv 0.1$, $i_n \equiv 0$ and $\psi_n \equiv 10$).

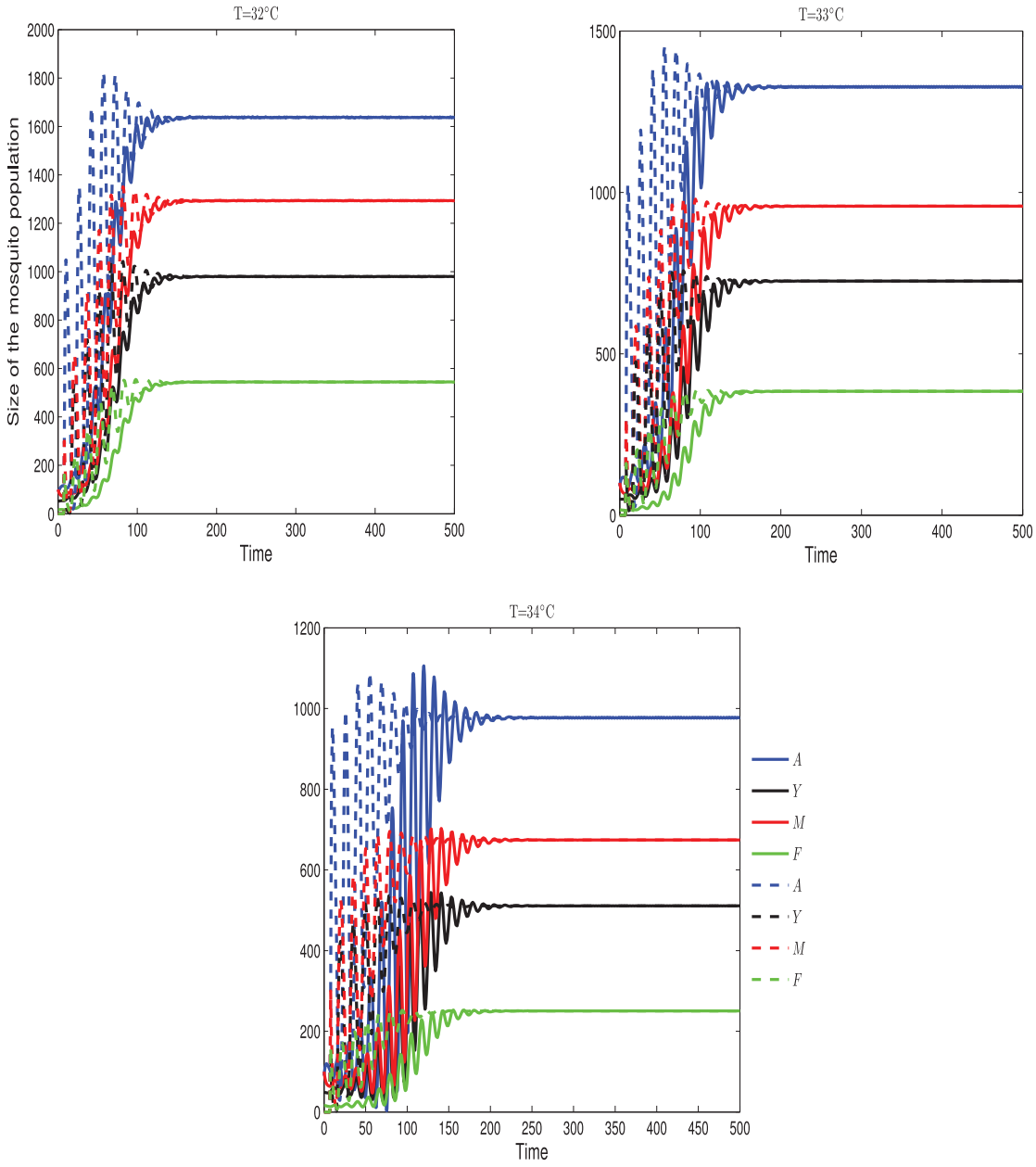

Fig. 12. The dynamical consistency between the delay differential system (solid curves)and the corresponding discrete model (dashed curves) under varying environmental temperatures (32 °C, 33°C and 34 °C). Here, $k = f = 0.9$, $\kappa = 0.6$, the other parameters being given in Table 2. When $T = 32\,^{\circ}$C, one finds that $\boldsymbol{X}_2^* = (1637.2, 979.8940, 1293.2, 544.4055)$ is locally stable. When $T = 33\,^{\circ}$C, one finds that $\boldsymbol{X}_2^* = (1326.8, 725.2508, 957.1717, 383.7121)$ is locally stable. When $T = 34\,^{\circ}$C, one finds that $\boldsymbol{X}_2^* = (977.0405, 510.7485, 674.0758, 250.4672)$ is locally stable. The initial conditions $A(0) = 90$, $t \in [-\tau, 0]$, $Y(0) = 50$, $M(0) = 100$ and $F(0) = 16$.

In addition, for the numerical simulations presented here, to illustrate the effect of the combined strategies on the growth of mosquito population of the aquatic phase, we shall consider that there exists a non-trivial steady state of the system (7)–(10), which is locally stable. We shall also use the following values for the variable parameters: $T = 24\,^{\circ}$C, 28 °C and 32 °C, time step size=5, $c_\alpha = 800$, $c_i = 10^4$, $c_\psi = 0.0138$, $N = 20$, $\alpha \in [0.1, 1]$, $i \in [0, 0.5]$ and $\psi \in [10, 100]$, and the following values for the initial state variables: $A(t) = 2000$, $t \in [-\tau(T), 0]$, $Y(0) = 800$, $M(0) = 1000$ and $F(0) = 300$.

6.1. Environmental temperature maximizing the capacity of breeding sites

Here, we first consider that the environmental temperature is 24 °C, at which the breeding sites are close to their maximal capacity, as indicated in Fig. 4. As shown in Figs. 2 and 5, the mean instar duration is short and the oviposition rate of immature

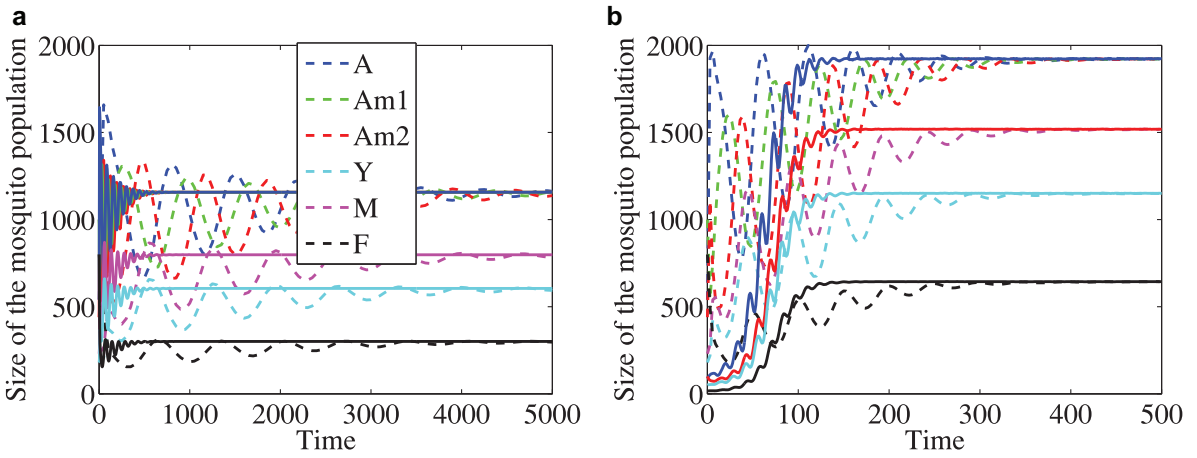

Fig. 13. The dynamical consistency between the transformed NSFD delay-free scheme (45) (dashed lines) and the continuous delay model (1)–(6) (solid lines). The initial conditions are $A(t) = 1000$, $A_{m1}(t) = 440$,$A_{m2}(t) = 5400$,$t \in [-\tau, 0]$, $Y(0) = 180$, $M(0) = 230$, $F(0) = 800$, $k = f = 0.9$, $\beta = 0.2643$ and $\kappa = 0.6$, the other parameters being as given in Table 2. Also, $h = 5$ and $T = 34\,^{\circ}$C for (a), while $h = 3$ and $T = 32\,^{\circ}$C for (b). It is observed that the solutions converge to their respective equilibrium values in each case.

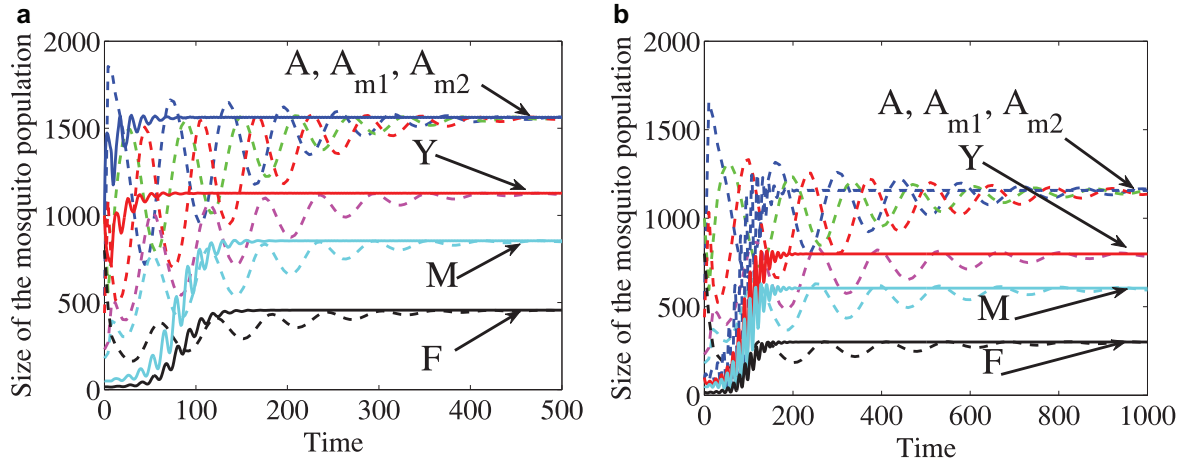

Fig. 14. The dynamical consistency between the transformed NSFD delay-free scheme (45) (dashed lines) and the continuous delay model (1)–(6) (solid lines). The initial conditions are $A(t) = 1000$, $A_{m1}(t) = 440$,$A_{m2}(t) = 5400$,$t \in [-\tau, 0]$, $Y(0) = 180$, $M(0) = 230$, $F(0) = 800$, $k = f = 0.9$, $\beta = 0.2643$ and $\kappa = 0.6$, the other parameters being as given in Table 2. Also, $h = 4$ for (a) and $h = 10$ for (b). It is observed that the equilibrium $\boldsymbol{X}_2^*$ converge to their respective equilibrium values in each case.

stages of *Aedes aegypti* is low as well. We also observe that the survival rate of the immature stages is high for this environmental temperature. Second, when considering $T = 28\,^{\circ}$C, the breeding sites are also close to their maximal capacity, as shown in Fig. 4. A comparison with the corresponding parameters obtained for $T = 24\,^{\circ}$C reveals that the survival rate of the immature stages increases slightly and the mean instar duration decreases slightly, but the oviposition rate increases 1.5 times. Initially, at the lower temperature $T = 24\,^{\circ}$C, all three controls are employed to optimize the objective function $\mathcal{V}_N$, as shown in Fig. 15. The optimal population size of the aquatic stage always oscillates since all controls are triggered to minimize $\mathcal{V}_N$. At the intermediate temperature $T = 28\,^{\circ}$C, initially, all three controls are employed to optimize the objective function $\mathcal{V}_N$. After an increase in the size of the aquatic population, overall pesticide use on the aquatic and adult stages has an oscillation of small amplitude and the amount of sterile mosquitoes released decreases and then keeps a lower level. Finally, the population size of the aquatic stage reaches a certain level with higher α, low i and lower ψ.

6.2. Higher environmental temperature

Considering the higher environmental temperature of 32 °C here, as shown in Figs. 4 and 5, we observe the smaller capacity of breeding sites, the shorter instar duration as well as the much higher oviposition rate of immature stages. Initially, all three controls are triggered to minimize $\mathcal{V}_N$. Finally, once the population size of the aquatic stage reaches a certain level, only two control variables (higher α and lower i) are used to minimize the objective function shown in Fig. 15. In addition, the numerical result shown in Fig. 16 shows that the oviposition rate of immature stages mainly determines the outcomes of mosquito control.

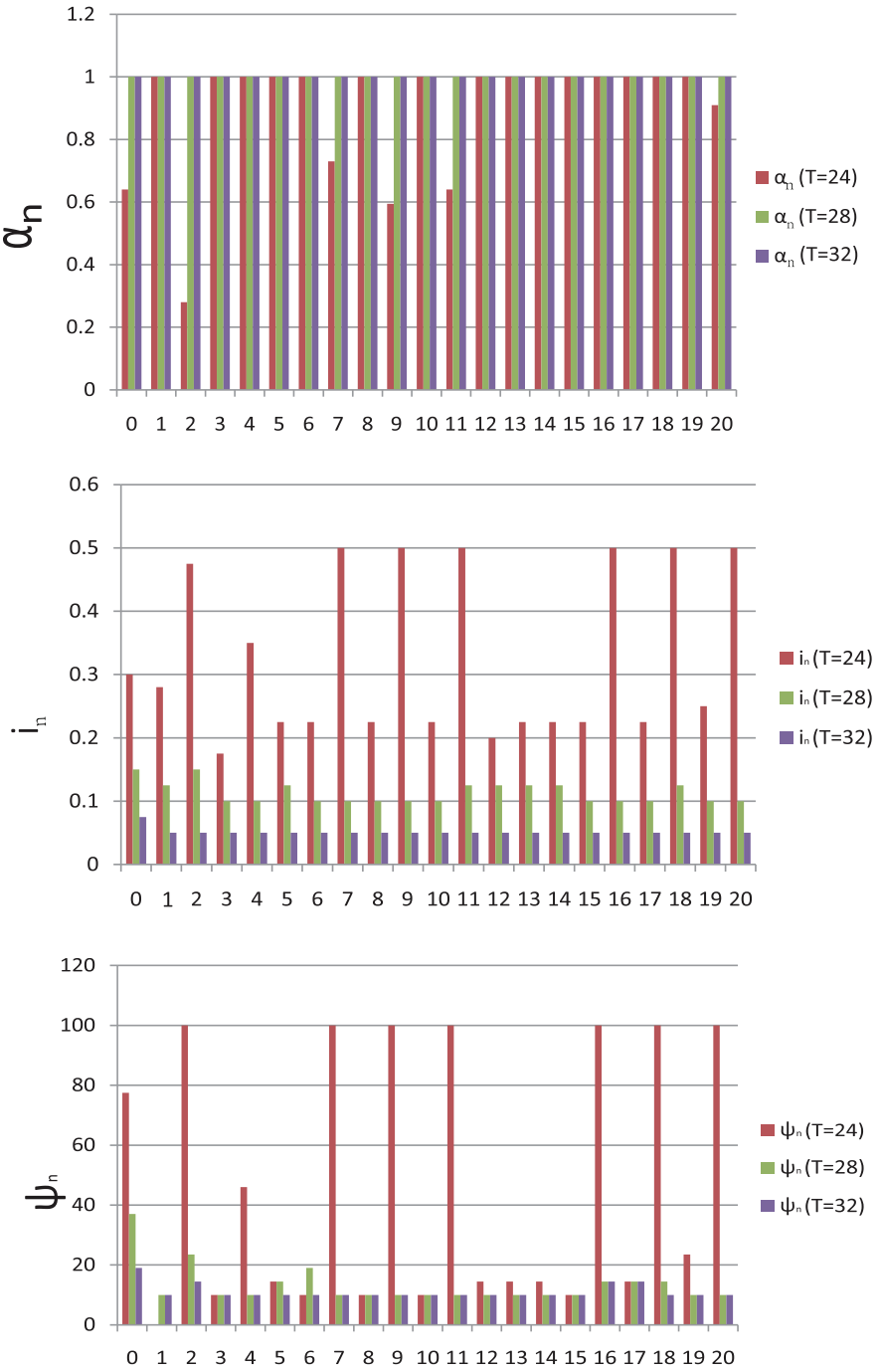

Fig. 15. Simulation showing the impact of varying the environmental temperature ($T = 24\,^{\circ}$C, $28\,^{\circ}$C and $32\,^{\circ}$C) upon the optimal control regimes. Here, $N = 20$, $k = f = 0.9$, $\kappa = 0.6$, the other parameters being given in Table 2. The initial conditions are $A(t) = 2000$, $t \in [-\tau, 0]$, $Y(0) = 800$, $M(0) = 1000$ and $F(0) = 300$.

7. Concluding remarks

The present paper attempts to formulate and study a delayed model for the dynamics of a mosquito population which is subject to three control mechanisms, namely to the release of pesticides, to the use of mechanical controls and, most importantly, to the sterile insect technique (SIT). The latter technique consists in the release of sterile male individuals with the purpose of interfering with the reproductive processes of the wild mosquitoes.

The existence of the positive equilibria is completely characterized in terms of two threshold parameters, being observed that the "richer" equilibrium (with more mosquitoes in the aquatic phase) has more chances to be stable, while a longer delay

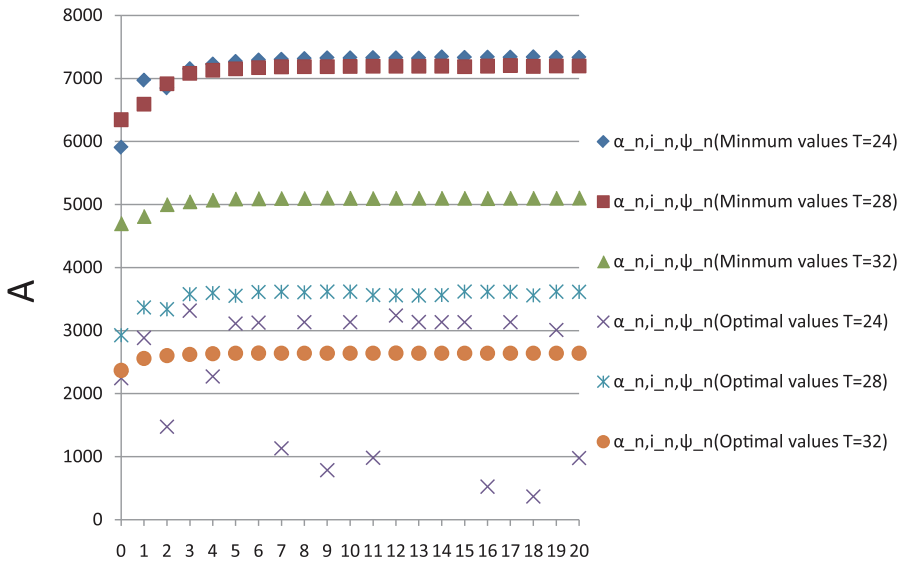

Fig. 16. Simulation showing the impact of varying the environmental temperature ($T = 24\,^{\circ}$C, $28\,^{\circ}$C and $32\,^{\circ}$C) and the population size of the aquatic phase upon the optimal combined control regime. Here, $N = 20$, $k = f = 0.9$, $\kappa = 0.6$, the other parameters being given in Table 2, and the initial conditions are $A(t) = 2000$, $t \in [-\tau, 0]$, $Y(0) = 800$, $M(0) = 1000$ and $F(0) = 300$.

(longer duration of the aquatic phase) has the potential to destabilize both positive equilibria, which become unstable for delays larger than certain values, after a finite number of stability switches. The stability of the trivial equilibrium appears to be more influenced by the value of the maturation rate from the aquatic phase to the adult phase, being observed that a small maturation rate attracts the stability of the trivial equilibrium. Also, if the maturation rate surpasses a certain threshold value, then the trivial equilibrium is stable if the delay is smaller than a certain value and unstable if the opposite inequality holds.

To preserve the positivity of the approximating solutions and to keep consistency with the continuous model, a nonstandard finite difference scheme is devised, the resulting discrete model being then transformed into a delay-free model by using the method of augmented states. The existence of optimal controls is investigated, a necessary condition in this sense being then determined.

Since the oviposition rate and the carrying capacity of the aquatic stage, as well as the mean instar duration, heavily depends on the environmental temperature, the particulars of different control regimes under varying environmental temperature are investigated by means of numerical simulations. It is observed that a combination of all three controls has the highest impact upon the size of the aquatic population, while at higher environmental temperatures the oviposition rate has the most prominent influence upon the outcome of the control measures.

Acknowledgments

The work of H.Z. was supported by the National Natural Science Foundation of China, Grant ID 11201187, the Scientific Research Foundation for the Returned Overseas Chinese Scholars and the China Scholarship Council. The work of P.G. was supported by a grant of the Romanian National Authority for Scientific Research, CNCS-UEFISCDI, project number PN-II-ID-PCE-2011-3-0557. A.S.H. acknowledges with thank the support of DST/NRF South African Research Chairs Initiative (SARChI) on Mathematical Models and Methods in Bioengineering and Biosciences (M^3B^2), MacArthur foundation grant, Bayero University, Kano, Nigeria and Centre of Excellence in Mathematics and Statistical Sciences (COE-Mass), South Africa.

References

[1] L. Alphey, C.B. Beard, P. Billingsley, M. Coetzee, A. Crisanti, C. Curtis, P. Eggleston, C. Godfray, J. Hemingway, M. Jacobs-Lorena, A.A. James, F.C. Kafatos, L.G. Mukwaya, M. Paton, J.R. Powell, W. Schneider, T.W. Scott, B. Sina, R. Sinden, S. Sinkins, A. Spielman, Y. Touré, F.H. Collins, Malaria control with genetically manipulated insect vectors, Science 298 (2002) 119–121.
[2] R. Anguelov, Y. Dumont, J.M.S. Lubuma, On non-standard finite difference schemes in biosciences, in: M.D. Todorov (Ed.), Proceedings of the 4th International Conference on Application of Mathematics in Technical and Natural Sciences, AIP Conf. Proc. 1487, 2012, pp. 212–223.
[3] R. Anguelov, J.M.S. Lubuma, Contribution to the mathematics of the nonstandard finite difference methods and applications, Numer. Methods Part. Differ. Equ. 17 (2001) 518–543.
[4] R. Anguelov, J.M.S. Lubuma, Nonstandard finite difference method by nonlocal approximation, Math. Comput. Simul. 61 (2003) 465–475.
[5] R. Anguelov, Y. Dumont, J. Lubuma, Mathematical modeling of sterile insect technology for control of anopheles mosquito, Comput. Math. Appl. 64 (2012) 374–389.

[6] R. Bellman, K.L. Cooke, Differential-Difference Equations, Academic Press, London, 1963.
[7] M.Q. Benedict, A.S. Robinson, The first releases of transgenic mosquitoes: an argument for the sterile insect technique, Trends Parasitol. 19 (2003) 349–355.
[8] J.G. Breman, The ears of the hippopotamus: manifestations, determinants, and estimates of the malaria burden, Am. J. Trop. Med. Hyg. 64 (2001) 1–11.
[9] J.H. Bryan, Results of consecutive matings of female *Anopheles gambiae* species B with fertile and sterile males, Nature 218 (1968) 489.
[10] L.-M. Cai, M. Martcheva, X.-Z. Li, Competitive exclusion in a vector-host epidemic model with distributed delay, J. Biol. Dyn. 7 (Suppl. 1) (2013) 47–67.
[11] M.R. Capeding, N.H. Tran, S.R.S. Hadinegoro, H.I.M. Ismail, T. Chotpitayasunondh, M.N. Chua, C.Q. Luong, K. Rusmil, D.N. Wirawan, R. Nallusamy, P. Pitisuttithum, U. Thisyakorn, I.-K. Yoon, D. van der Vliet, E. Langevin, T. Laot, Y. Hutagalung, C. Frago, M. Boaz, T.A. Wartel, N.G. Tornieporth, M. Saville, A. Bouckenooghe, and the CYD14 Study Group Clinical efficacy and safety of a novel tetravalent dengue vaccine in healthy children in Asia: a phase 3, randomised, observer-masked, placebo-controlled trial, Lancet 384 (2014) 1358–1365.
[12] C.L. Chen, D.Y. Sun, C.Y. Chang, Numerical solution of time-delayed optimal control problems by iterative dynamic programming, Optim. Control Appl. Methods 21 (2000) 91–105.
[13] N. Chitnis, J.M. Hyman, J.M. Cushing, Determining important parameters in the spread through the sensitivity analysis of a mathematical model, Bull. Math. Biol. 70 (2008) 1272–1296.
[14] K.L. Cooke, P. van den Driessche, On zeros of some transcendental equations, Funkc. Ekvacioj 29 (1986) 77–90.
[15] K.L. Cooke, P. van den Driessche, X. Zou, Interaction of maturation delay and nonlinear birth in population and epidemic models, J. Math. Biol. 39 (1999) 332–352.
[16] S. Dadebo, R. Luus, Optimal control of time-delay systems by dynamic programming, Optim. Control Appl. Methods 13 (1992) 29–41.
[17] H. Diaz, A.A. Ramirez, A. Olarte, C. Clavijo, A model for the control of malaria using genetically modified vectors, J. Theor. Biol. 276 (2011) 57–66.
[18] D.T. Dimitrov, H.V. Kojouharov, B.M. Chen, Reliable finite difference schemes with applications in mathematical ecology, in: R.E. Mickens (Ed.), Advances in the Applications of the Nonstandard Finite Difference Schemes, World Scientific Publishing, River Edge, NJ, 2005, pp. 249–286.
[19] C. Dufourd, Y. Dumont, Impact of environmental factors on mosquito dispersal in the prospect of sterile insect technique control, Comput. Math. Appl. 66 (2013) 1695–1715.
[20] Y. Dumont, J.M. Tchuenche, Mathematical studies on the sterile insect technique for the Chikungunya disease and *Aedes albopictus*, J. Math. Biol. 65 (2012) 809–854.
[21] Y. Dumont, F. Chiroleu, Vector control for the Chikungunya disease, Math. Biosci. Eng. 7 (2010) 315–348.
[22] L. Esteva, H.M. Yang, Mathematical model to assess the control of *Aedes aegypti* mosquitoes by the sterile insect technique, Math. Biosci. 198 (2005) 132–147.
[23] G. Fan, J. Liu, P. van den Driessche, J. Wu, H. Zhu, The impact of maturation delay of mosquitoes on the transmission of West Nile virus, Math. Biosci. 228 (2010) 119–126.
[24] K.R. Fister, M.L. McCarthy, S.F. Oppenheimer, C. Collins, Optimal control of insects through ste\rile insect release and habitat modification, Math. Biosci. 44 (2013) 201–212.
[25] S.M. Garba, A.B. Gumel, A.S. Hassan, J.M.-S. Lubuma, Switching from exact scheme to nonstandard finite difference scheme for linear delay differential equation, Appl. Math. Comput. 258 (2015) 388–403.
[26] S.M. Garba, A.B. Gumel, J.M.-S. Lubuma, Dynamically-consistent non-standard finite difference method for an epidemic model, Math. Comput. Model. 53 (2011) 131–150.
[27] P. Georgescu, Y.H. Hsieh, Global dynamics for a predator-prey model with stage structure for predator, SIAM J. Appl. Math. 67 (2007) 1379–1395.
[28] G.C. Goodwin, M.M. Seron, J.D. Doná, Constrained Control and Estimation: An Optimisation Approach, Springer-Verlag London Limited, 2005.
[29] D.J. Gubler, Dengue, in: T.P. Monath (Ed.), The Arboviruses: Epidemiology and Ecology vol. II , CRC, Boca Raton, FL, 1986, p. 213.
[30] D.J. Gubler, The changing epidemiology of yellow fever and dengue, 1900 to 2003: full circle? Comp. Immunol. Microbiol. Infect. Dis. 27 (2004) 319–330.
[31] D.J. Gubler, M. Meltzer, Impact of dengue/dengue hemorrhagic fever on the developing world, Adv. Virus Res. 53 (1999) 35–70.
[32] J. Guckenheimer, P. Holmes, Nonlinear Oscillations, Dynamical Systems, and Bifurcations of Vector Fields, Springer Verlag, Berlin, 1983.
[33] M.E.H. Helinski, M.M. Hassan, W.M. El-Motasim, C.A. Malcolm, B.G.J. Knols, B. El-Sayed, Towards a sterile insect technique field release of *Anopheles arabiensis* mosquitoes in Sudan: Irradiation, transportation, and field cage experimentation, Malar. J. 7 (65) (2008).
[34] J.K. Hale, Introduction to Functional Differential Equations, Springer-Verlag, New York, 1993.
[35] J. Henderson, R. Luca, Boundary Value Problems for Systems of Differential, Difference and Fractional Equations, Elsevier, 2015.
[36] http://www.who.int/denguecontrol/mosquito/en/. (accessed January, 2014).
[37] E.F. Knipling, Possibilities of insect control or eradication through the use of sexually sterile males, J. Econ. Entomol. 48 (1955) 459–462.
[38] E.F. Knipling, Sterile insect technique as a screwworm control measure: the concept and its development, in: O.H. Graham (Ed.), Symposium on Eradication of the Screwworm from the United States and Mexico, Misc. Publ. Entomol. Soc. America, 62, College Park, MD, 1985, pp. 4–7.
[39] E.F. Knipling, The basic principles of insect population suppression and management, Agriculture Handbook, U.S. Dept. of Agriculture, Washington, DC, 1979, vol. 512.
[40] Y. Kuang, Delay Differential Equations with Applications in Population Dynamics, Academic Press, Boston, 1993.
[41] J. Li, Differential equations models for interacting wild and transgenic mosquito populations, J. Biol. Dyn. 2 (2008) 241–258.
[42] J. Li, Simple mathematical models for interacting wild and transgenic mosquito populations, Math. Biosci. 189 (2004) 39–59.
[43] W.T. Lin, T.R. Burkot, B.H. Kay, Effects of temperature and larval diet on development rates and survival of the dengue vector *Aedes aegypti* in north Queensland, Australia, Med. Vet. Entomol. 14 (2000) 31–37.
[44] N. Liu, Q. Xu, F. Zhu, L. Zhang, Pyrethroid resistance in mosquitoes, Insect Sci. 13 (2006) 159–166.
[45] X. Liu, P. Stechlinski, Application of control strategies to a seasonal model of Chikungunya disease, Appl. Math. Modell. 39 (2015) 3194–3220.
[46] N.A. Maidana, H.M. Yang, Describing the geographic propagation of dengue disease by travelling waves, Math. Biosci. 215 (2008) 64–77.
[47] R.E. Mickens, Calculation of denominator functions for nonstandard finite difference schemes for differential equations satisfying a positivity condition, Numer. Methords Part. Differ. Equ. 23 (2007) 672–691.
[48] R.E. Mickens, Nonstandard Finite Difference Models of Differential Equations, World Scientific, 1994.
[49] G.M.L. Nayyar, J.G. Breman, P.N. Newton, J. Herrington, Poor-quality antimalarial drugs in southeast Asia and sub-Saharan Africa, Lancet Infect. Dis. 12 (2012) 488–496.
[50] G.A. Ngwa, A.M. Niger, A.B. Gumel, Mathematical assessment of the role of non-linear birth and maturation delay in the population dynamics of the malaria vector, Appl. Math. Comput. 217 (2010) 3286–3313.
[51] R. Norrby, Outlook for a dengue vaccine, Clin. Microbiol. Infect. 20 (Suppl. 5) (2014) 92–94.
[52] C.F. Oliva, M. Jacquet, J. Gilles, G. Lemperiere, P.O. Maquart, S. Quilici, F. Schooneman, M.J.B. Vreysen, S. Boyer, The sterile insect technique for controlling populations of *Aedes albopictus* (*Diptera: Culicidae*) on Reunion island: mating vigour of sterilized males, PLoS One 7 (2012) e49414.
[53] G. Pialoux, B.-A. Gaüzère, S. Jauréguiberry, M. Strobel, Chikungunya, an epidemic arbovirosis, Lancet Infect. Dis. 7 (2007) 319–327.
[54] M. Rafikov, A.P.P. Wyse, L. Bevilacqua, Controlling the interaction between wild and transgenic mosquitoes, J. Nonlinear Syst. Appl. (2010) 27–30.
[55] M. Rafikov, L. Bevilacqua, A.P.P. Wyse, Optimal control strategy of malaria vector using genetically modified mosquitoes, J. Theor. Biol. 258 (2009) 418–425.
[56] G.B. Schaalje, Dynamical models of pesticide effectiveness, Environ. Entomol. 19 (1990) 439–447.
[57] J. Thailayil, K. Magnusson, H.C.J. Godfray, A. Crisanti, F. Catteruccia, Spermless males elicit large-scale female responses to mating in the malaria mosquito *Anopheles gambiae*, Proc. Natl. Acad. Sci. USA 108 (2011) 13677–13681.
[58] The RTS,S Clinical Trials Partnership, Efficacy and Safety of the RTS,S/AS01Malaria vaccine during 18 months after vaccination: a phase 3 randomized, controlled trial in children and young infants at 11 African sites, PLoS Med. 11 (2014) e1001685.
[59] C. Vargas-De-León, L. Esteva, A. Korobeinikov, Age-dependency in host-vector models: the global analysis, Appl. Math. Comput. 243 (2014) 969–981.
[60] H.J. Wearing, Ecological and immunological determinants of dengue epidemics, Proc. Natl. Acad. Sci. USA 103 (2006) 11802–11807.
[61] S.C. Weaver, J.E. Osorio, J.A. Livengood, R. Chen, D.T. Stinchcomb, Chikungunya virus and prospects for a vaccine, Expert Rev. Vaccines 11 (2012) 1087–1101.

[62] H.-M. Wei, X.-Z. Li, M. Martcheva, An epidemic model of a vector-borne disease with direct transmission and time delay, J. Math. Anal. Appl. 342 (2008) 895–908.
[63] K.J. Wilby, T.T.Y. Lau, S.E. Gilchrist, M.H.H. Ensom, Mosquirix (RTS,S): a novel vaccine for the prevention of *Plasmodium falciparum* malaria, Ann. Pharmacother. 46 (2012) 384–393.
[64] A.B.B. Wilke, D.D. Nimmo, O. St John, B.B. Kojin, M.L. Capurro, M.T. Marrelli, Mini-review: genetic enhancements to the sterile insect technique to control mosquito populations, Asia-Pac. J. Mol. Biol. Biotechnol. 17 (2009) 65–74.
[65] H.M. Yang, M.L.G. Macoris, K.C. Galvani, M.T.M. Andrighetti, D.M.V. Wanderley, Assessing the effects of temperature on the population of *Aedes aegypti*, the vector of dengue, Epidemiol. Infect. 137 (2009) 1188–1202.